

Università degli Studi di Napoli Federico II



**DOTTORATO DI RICERCA IN
FISIOPATOLOGIA CLINICA E MEDICINA SPERIMENTALE**

Indirizzo in Scienze Gerontologiche

XXVIII ciclo

Coordinatore: Prof. Gianni Marone

TESI DI DOTTORATO

**The use of new echocardiographic technologies
in study of myocardial function**

Tutor

Prof. Giovanni de Simone

Candidato

Dott.ssa Roberta Esposito

Index

First Study: Background	4
First Study:.....	4
Abstract	4
Introduction.....	5
Methods.....	6
Results.....	10
Discussion	11
References.....	14
Figures.....	19
Tables	24
Second Study: Background.....	28
Second Study:	28
Abstract	28
Introduction.....	29
Methods.....	30
Results.....	33
Discussion	34
References.....	12
Figures.....	45

Tables	46
Third Study: Background.....	50
Third Study:	50
Abstract	50
Methods.....	52
Results.....	55
Discussion	57
References.....	59
Tables	64
Figures.....	66

First Study: Background

The thesis collects research conducted during the doctoral period. The first research is a pathophysiological study on athlete's heart and particularly on right ventricular function, myocardial instrumental in the athlete's performance. The study involved the use of new echocardiographic technologies, Speckle Tracking Echocardiography and three-dimensional echo. Were compared 43 healthy sedentary subjects and 40 top-level athletes, all subjects were studied with standard echocardiography and with new echocardiographic technologies. There were no significant differences between the 2 groups with regard to the Doppler parameters, while the athletes had volumes (end-diastolic and end-systolic) larger without significant differences in ejection fraction. Longitudinal strain of the right ventricle, both the global and lateral wall it appeared higher in athletes, and there was a close correlation between the lateral longitudinal strain and the diastolic volume after adjustment for heart rate. We concluded that the determinants of supernormal function of the right ventricle can be very well identified by a combined study of the right ventricle with Speckle Tracking and three-dimensional echocardiography. The preload of the right ventricle does its utmost influence on the lateral longitudinal fibers, this effect results in an increase in stroke volume of the right ventricle. This study, which is the text in full, was published in *Echocardiography* (2014 Sep; 31 (8): 996-1004).

First Study:

Prominent contribution of free wall to supernormal right ventricular function in the athlete's heart: combined assessment by Speckle Tracking and three-dimensional echocardiography

Abstract

The aim was to assess determinants of right ventricular (RV) function in top-level athletes by Speckle Tracking (STE) and real-time 3D echocardiography (RT3DE). RV function of 43 sedentary

normals and 40 top-level rowers was compared by standard echo-Doppler, RT3DE and STE. RV diameters, tricuspid annular plane systolic excursion (TAPSE), tricuspid E/A ratio and pulsed Tissue Doppler of lateral tricuspid annulus were analyzed. RV volumes, ejection fraction (EF) and stroke volume (SV) were determined by RT3DE. STE-derived RV global longitudinal strain (GLS) (average of 6 segments), septal strain (average of 3 septal regions, SLS) and lateral strain (average of 3 lateral regions, LLS) were estimated by STE. The 2 groups were comparable for age, body mass index and blood pressure but heart rate (HR) was lower in rowers. RV diameters were larger and TAPSE, E/A ratio, and Tissue Doppler derived s' and e' velocities higher in rowers. RT3DE RV end-diastolic volume (EDV) and end-systolic volume were greater in rowers (both $p < 0.0001$), without EF difference. GLS ($p < 0.005$) and LLS ($p < 0.001$), but not SLS, were higher in rowers. In the pooled population LLS was related to EDV and SV, even after adjusting for HR ($r = 0.35$, $p < 0.001$ and $r = 0.33$, $p < 0.002$ respectively). Determinants of supernormal RV function of athletes can be identified by the combination of RT3DE and STE. RV preload exerts its maximal influence on the longitudinal lateral fibers, whose effect induces in its turn the increase of stroke volume.

Key Words: Athlete's heart, Right ventricle, Speckle Tracking Echocardiography, Longitudinal strain, Three-dimensional echocardiography

Introduction

Intensive endurance training in competitive athletes leads to cardiac morphological and functional changes that become gradually overt and disappear stopping the sport activity. The "athlete's heart" includes symmetrical and shapely increase in internal diameters and wall thickness of atrial and ventricular chambers [1-5]. Their final size could vary in dependence of type, intensity and duration of competitions and training sessions, individual physiological features (largely genetically defined)

and age at the time of training begin. While a large number of studies has been published on left ventricular (LV) features produced by intensive training, mainly LV hypertrophy [6-8], little is known about right ventricular (RV) morphology and function of the “athlete’s heart”.

RV dysfunction is a recognized index of functional capacity as well as a survival predictor in several clinical conditions [9,10]. Nevertheless, the right ventricle has been long defined as the “forgotten” cardiac chamber, an expression which points out its poor knowledge and is mainly related to its difficult ultrasound approach. This is due to its difficult location (just behind the breastbone, forward the left ventricle) [11] and its complex shape which includes three main portions: inflow tract (inlet), outflow tract (outlet), and a trabeculated muscular apex [12,13]. The localization of inflow and outflow tracts at two different levels makes RV internal volume to be unrelated to any geometric assumption. Recent development in ultrasound technology now allows a complete assessment of RV volumes and ejection fraction (EF) by real-time three-dimensional echocardiography (RT3DE) which enables this technique to compete with cardiac magnetic resonance imaging (MRI) [14,15]. On the other hand, two-dimensional Speckle Tracking Echocardiography (STE) makes possible the assessment of RV regional and global longitudinal deformation [16,17]. Differently from the left ventricle, RV myocardial fibers arrangement is predominantly longitudinal and RV contraction is mainly due to longitudinal shortening [12]. In this view, STE-derived longitudinal strain can be very powerful diagnostic for RV functional assessment.

The present study was designed to assess determinants of supernormal RV contractility in competitive athletes by combining the two novel technologies of RT3DE and STE.

Methods

Study Population

The study population included male Italian top-level rowers (performing competitive activity for a period ranging from 4 to 12 years), consecutively visited in our Department under a written invitation forwarded to famous Nautical Associations of Naples and a control group of sedentary healthy normals recruited from the personnel of our university and their relatives involved in a screening prevention program. To be eligible, athletes had to be engaged in a mixed training program (isotonic and isometric) of at least 30 h per week in the last 4 years. They were examined during an intense training period, at least 24 h after last athletic activity. All participants gave written informed consent to the procedures before entering the study. They were judged to be free of cardiac disease on the basis of negative medical history, normal physical examination, 12-lead ECG, and Doppler echocardiographic examination. Blood pressure was < 140/90 mmHg in each subject. None had any disease or injury in the 4 weeks prior to the beginning of the study, nor were taking any medication, abusive substances (including anabolic steroids and GH), alcohol or smoking. After the exclusions, the study population included 40 athletes top-level rowers and 43 healthy controls.

Procedures

The echocardiographic examinations were performed using a Vivid E9 ultrasound scanner (GE Healthcare, Milwaukee, WI, USA). Heart rate and blood pressure (BP) (average of three measurements by a cuff sphygmomanometer) were measured at the end of the examination. Images acquisition and measurements determination of both conventional and advanced techniques (RT3DE and STE) were done according to standardized procedures [18-20].

Standard echocardiographic examination. Standard echo examination was performed using a 2.5 MHz transducer with harmonic capability according to the standards of our laboratory [18-20]. RV global systolic function was assessed as tricuspid annular systolic excursion (TAPSE, mm) by M-

mode scanning of the lateral tricuspid annulus. In apical 4-chamber view pulsed Doppler RV inflow assessment was recorded to measure early diastolic (E) and atrial (A) peak velocities (m/sec) and E/A ratio at the tips of the tricuspid leaflets, and pulsed Tissue Doppler of the lateral tricuspid annulus to measure systolic (s'), early diastolic (e') and atrial (a') velocities (all in cm/sec) [21]. In the parasternal short-axis view of the great vessels pulsed Doppler of RV outflow tract was recorded and both pre-ejection period (RV PEP) and ejection time (RV ET) (both in msec) measured as parameters of RV systolic function.

RT3DE. RT3DE data set acquisition of the left ventricle obtained using a 3D volumetric transducer. A full-volume RV scan was acquired from the apical approach using harmonic imaging, with adjustment of image contrast, frequency, depth and sector size for adequate frame-rate and optimal RV border visualization. Tricuspid valve, but not entire right atrium, was included in the data set throughout the cardiac cycle. Gain was set higher than for usual 2-D images [21]. Respiratory maneuvers were applied for optimizing endocardial border visualization, especially when RV anterior wall could not be otherwise encompassed in the data set. Then, consecutive 4-beat ECG-gated sub-volumes were acquired during breath holding to generate the full-volume data set. Operators were requested to perform quality check by 2D RV multiplane display and 3D RV transversal plane during acquisition (**Figure 1**) as well as by 9-slice display immediately after acquisition (**Figure 1**). Adequate 3D data sets of the right ventricle were stored digitally in raw-data format. The software which provides 3D measurements of RV function (4D-RV function, version 2.6, TomTec Imaging Systems, Gmbh, Unterschleissheim, Germany) is clinically validated against cardiac MRI [14,15]. Every RV full-volume 3-D data set is automatically cropped in 3 standard planes (views): 4-chamber, coronal and sagittal. After optimizing each view according to anatomical landmarks (RV inflow and outflow), 3-D data sets can be manipulated by the reader with a series of translational, rotational and pivoting manoeuvres, for the reference line to pass

through the center of tricuspid valve and RV apex in each view. End-diastolic (largest RV area) and end-systolic (smallest area) frames are then manually set in 4-chamber view. Point identification for mitral and tricuspid valve and LV apex are required. In the assessment of the present study readers were required to trace endocardial border at end-diastole and end-systole for the 3 selected RV planes. Care was taken to trace endocardial border just outside the blood-tissue interface and papillary muscles, moderator band and endocardial trabeculae were included in RV cavity. These manually traced contours served for initiation of automated border detection algorithm. Frame-by-frame correction of endocardial border was applied when needed. Measurements of RV end-diastolic volume (EDV), end-systolic volume (ESV) and ejection fraction (EF) and stroke volume (SV) and cardiac output were finally obtained (**Figure 2**). Additional measurements of RT3DE included LV mass and LV mass index ($\text{g/m}^{2.7}$) which were obtained according to the standards of our laboratory [20].

Speckle Tracking Echocardiography. STE of the right ventricle was performed by recording an apical 4-chamber view according to a previously validated method, whose reproducibility has been previously reported [17]. Reliable recording of 2D images for STE requires a high frame rate (40-70 frames/s), without dual focusing. To achieve this goal it is necessary to record RV cavity with the narrowest scan and at the lowest possible depth in order to display on the screen the left ventricle as large as possible. Care was also taken to obtain the best visualization of the right ventricle, such to obtain the best delineation of endocardial borders. Custom acoustic-tracking software was applied on 2D gray-scale images by tracking movements of “speckles” in the myocardial tissue, frame by frame throughout the cardiac cycle. The software is interactive (endocardial-cavity interface traced manually and epicardial tracing generated automatically) and rejects poorly tracked segments, allowing the observer to manually override its decision by visual assessment. The reading analysis was performed using a commercially available semi-automated 2D strain software in a dedicated

workstation (Echopac, GE). After the segmental tracking quality analysis and the eventual manual adjustment of the endocardial borders, the longitudinal strain curves were automatically generated for 6 RV regions of interest, 3 of free lateral wall and 3 of interventricular septum (**Figure 3**). Peak negative longitudinal strain was measured from the 6 segments. RV GLS was calculated by averaging values of the 6 segments. Segments with suboptimal tracking were excluded by the average. In addition, lateral longitudinal strain (LLS) was calculated as the average of the 3 regions of interest of the lateral wall and septal longitudinal strain (SLS) as the average of the 3 septal regions of interest.

Statistical Analysis

Statistical analysis was performed by SPSS package, release 12 (SPSS, Inc., Chicago, IL, USA). Data are presented as mean value + standard deviation (SD). Descriptive statistics was obtained by one-factor ANOVA and χ^2 distribution with computation of exact p-value by the Monte Carlo method. Least squares linear regression was used to evaluate univariate correlates of a given variable. The null hypothesis was rejected at $p \leq 0.05$.

Results

The characteristics of study population are listed in **Table 1**. The 2 groups were comparable for sex prevalence, age, body mass index and BP whereas heart rate was significantly lower in athletes than in controls ($p < 0.0001$).

Standard Doppler echocardiographic analysis of the right ventricle is summarized in **Table 2**. RV diameters were significantly larger ($p < 0.001$), and TAPSE ($p < 0.001$), tricuspid inflow E/A ratio ($p < 0.005$) as well as pulsed Tissue Doppler derived s' and e' velocities (both $p < 0.002$) higher in rowers while RV E/e' ratio did not differ between the 2 groups.

RT3DE analysis (**Table 3**) showed greater RV EDV and ESV in rowers (both $p < 0.0001$), without significant difference in EF between the 2 groups .

Table 4 reports STE results. Longitudinal strain of each of the 6 RV regional segments was significantly higher in athletes than in controls ($p < 0.005$). LLS was significantly higher in rowers ($p < 0.0001$) while SLS did not differ in comparison with the control group.

Table 5 shows univariate correlations of STE parameters in the pooled population. RV LLS, but not GLS nor SLS, was significantly related with both RV EDV and SV (**Table 6 (Figure 4)**). These relations remained significant even after adjusting for heart rate ($r = 0.35$, $p < 0.001$ and $r = 0.33$, $p < 0.002$ respectively).

Discussion

The present study demonstrates the additional value of new ultrasound technologies in defining the features of the athlete's heart. In absence of significant difference in RT3DE-derived EF in comparison with the control group, GLS and LLS were significantly higher in rowers. LLS was independently associated with EDV, a reliable marker of RV pre-load, and with SV. i.e. a true indicator of RV pump function.

Previous studies used pulsed Tissue Doppler to assess RV myocardial function in the supernormal athlete's heart [7,8,16,22]. These studies showed an increase of both RV systolic and early diastolic velocities as well as a prolongation of myocardial relaxation time, the latter two parameters being an expression of improved myocardial relaxation.

New ultrasound technologies, such as RT3DE and STE, have already demonstrated to allow more accurate and reliable assessment of RV morphology and function in different clinical scenarios [15,16,23-28]. The peculiarity of the present study was the choice of a combined evaluation of the right ventricle by using STE, which allows accurate assessment of global and regional RV

myocardial longitudinal function, and RT3DE, which makes possible a feasible and reliable determination of RV volumes and EF [14,15]. Normal values of RV size and function by 3RTDE have been also determined in the clinical setting [29].

STE of the right ventricle has been already applied to the athlete's heart. Recently D'Andrea et al. [27] demonstrated that, without difference of TAPSE obtained by M-mode assessment, RV GLS is substantially increased in endurance athletes in comparison with the sedentary controls. These results point out a training-induced improvement of RV longitudinal deformation which is detectable by STE but not by standard echocardiographic assessment. These authors also showed that LV end-diastolic diameter is an independent determinant of RV GLS, a finding which highlights an optimal cooperation between the two ventricles in athletes.

The present study extends the knowledge of RV physiology of the super-trained heart. We confirmed the increase of RV GLS in the athlete's heart since it was higher in rowers than in controls. Supernormal RV function appears therefore to be mainly sustained by the systolic deformation of longitudinal fibers. This is consistent with the assumption that RV systolic function involves mainly the contraction of longitudinal fibers which shortens the long axis and draws the tricuspid annulus towards the apex [12]. Of interest, the increased RV strain of our athletes was found to be associated to increase of RV (both end-diastolic and end-systolic) but in absence of changes in RV EF, this finding being in agreement with the concept that modifications of longitudinal deformation occur early than those involving chamber function. A mismatch between RV chamber function (normal) and longitudinal function (reduced as measured by TAPSE) was observed also in pathologic conditions such as in patients with mitral valve prolapse who had undergone cardiac surgery [30].

To the best of our knowledge, the present study is the first to observe that the increased RV strain of athletes is predominantly due to the contribution of RV lateral wall. In fact, lateral strain, but not

septal strain, was significantly increased in our rowers. The prominent contribution of RV lateral wall to the supernormal contractility could be expected since interventricular septum is also involved in LV function. Under normal loading and electrical conditions the septum is concave toward the left ventricle in both systole and diastole, more prone therefore to LV mechanics participation [12]. Conversely, RV lateral wall is free to exert all its action on RV systolic function. Of interest, the main contribution of RV lateral strain to RV mechanics was recently found in patients after heart transplantation [17].

It is also worthy of note that LLS was significantly related to both RT3DE-derived RV EDV and RV SV, markers of RV preload and LV pump function respectively. This results is a practical demonstration of the Frank-Starling mechanism applied to RV chamber: the greater RV EDV the better contractility of RV longitudinal fibers of the lateral wall induced by the optimal stretching of myocardial fibers, the better RV systolic performance. Similar findings were previously observed by the use of simple pulsed Tissue Doppler in competitive swimmers who showed positive associations of increased e' velocity of lateral tricuspid annulus with both greater RV end-diastolic diameter (preload) and increased SV (pump function) [7].

Study limitations. Since a definite STE software for RV 2D-strain has not yet been created, we applied STE technique of the left ventricle to analyze RV regional and global strain. This can be considered as a limitation [31] although both feasibility and reproducibility of RV strain patterns and measurements are well recognized in the clinical setting [17].

In conclusion, the combination of RT3DE and STE allows to increase the knowledge of determinants of RV function in rowers. Our findings demonstrate that, in absence of EF changes, RV global longitudinal function is increased, this increase being mainly due to the contribution of lateral wall contraction. RV preload increase (EDV) may be responsible of RV supernormal

contractility in rowers since it could induce the increased RV strain deformation of the lateral wall which in turn leads to a beneficial effect of global systolic performance (SV).

References

1. Vos M, Hauser AM, Dressendorfer RH, Hashimoto T, Dudley P, Gordon S, Timmis GC. Enlargement of the right heart in the endurance athlete: a two-dimensional echocardiographic study. *Int J Sports Med* 1985;6:271–275.
2. Rawlins J, Bhan A, Sharma S. Left ventricular hypertrophy in athletes. *Eur J Echocardiogr* 2009;10:350–356.
3. Douglas PS, O'Toole ML, Hiller WD, Reichek N. Different effects of prolonged exercise on the right and left ventricles. *J Am Coll Cardiol* 1990;15:64–69.
4. Henriksen E, Landelius J, Kangro T, Jonason T, Hedberg P, Wesslén L, Rosander, CN, Rolf C, Ringqvist I, Friman G, Wesslén L. An echocardiographic study of right and left ventricular adaptation to physical exercise in elite female orienteers. *Eur Heart J* 1999;20:309–316.
5. Erol MK, Karakelleoglu S. Assessment of right heart function in the athlete's heart. *Heart Vessels* 2002;16:175–180.
6. Caso P, Galderisi M, D'Andrea A, Di Maggio D, De Simone L, Martiniello AR, Mininni N, Calabrò R, Sutherland GR. Analysis by Doppler tissue imaging of ventricular interaction in long-distance competitive swimmers. *Am J Cardiol* 2002;90:193–197.
7. D'Andrea A, Caso P, Sarubbi B, Limongelli G, Liccardo B, Cice G, D'Andrea L, Scherillo M, Cotrufo M, Calabrò R. Right ventricular adaptation to different training protocols. *Echocardiography* 2003;20:329–336.
8. D'Andrea A, Caso P, Scarafilo R, Salerno G, De Corato G, Mita C, Di Salvo G, Allocca F, Colonna D, Caprile M, Ascione L, Cuomo S, Calabrò R. Biventricular myocardial

- adaptation to different training protocols in competitive master athletes. *Int J Cardiol* 2007;115:342–349.
9. Horton KD, Meece RW, Hill JC. Assessment of the right ventricle by echocardiography: a primer for cardiac sonographer. *J Am Soc Echocardiogr* 2009;22:776-792.
 10. Haddad F, Ashley E, Michelakis ED. New insight for diagnosis and management of right ventricular failure, from molecular imaging to targeted right ventricular therapy. *Curr Opin Cardiol* 2010;25:131-140.
 11. Levine RA, Gibson TC, Aretz T, Gillam LD, Guyer DE, King ME, Weyman AE. Echocardiographic measurement of right ventricular volume. *Circulation* 1984;69:497-505.
 12. Haddad F, Hunt S, Rosenthal DN, Murphy DJ. Right ventricular function in cardiovascular disease. Part I. Anatomy, physiology, aging and functional assessment of the right ventricle. *Circulation* 2008;117:1436-1448.
 13. Chin KM, Coghlan G. Characterizing the right ventricle: advancing our knowledge. *Am J Cardiol* 2012;110:3S-8S.
 14. Niemann PS, Pinho L, Balbach T, Galuschky C, Blankenhagen M, Silberbach M, Broberg C, Jerosch-Herold M, Sahn DJ. Anatomically oriented right ventricular volume measurements with dynamic three-dimensional echocardiography validated by 3-Tesla magnetic resonance imaging. *J Am Coll Cardiol* 2007;50:1668-1676.
 15. Leibundgut G, Rohner A, Grize L, Bernheim A, Kessel-Schaefer A, Bremerich J, Zellweger M, Buser P, Handke M. Dynamic assessment of right ventricular volumes and function by real-time three-dimensional echocardiography: a comparison study with magnetic resonance imaging in 100 adult patients. *J Am Soc Echocardiogr* 2010;23:116-126.

16. Meris A, Faletra F, Conca C, Klersy C, Regoli F, Klimusina J, Penco M, Pasotti E, Pedrazzini GB, Moccetti T, Auricchio A. Timing and magnitude of regional right ventricular function: a speckle tracking-derived strain study of normal subjects and patients with right ventricular dysfunction. *J Am Soc Echocardiogr* 2010;23:823-831.
17. Cameli M, Lisi M, Righini FM, Tsioulpas C, Bernazzali S, Maccherini M, Sani G, Ballo P, Galderisi M, Mondillo S. Right ventricular longitudinal strain correlates well with right ventricular stroke work index in patients with advanced heart failure referred for heart transplantation. *J Card Fail* 2012;18:208-215.
18. Cicala S, Galderisi M, Caso P, Petrocelli A, D'Errico A, de Divitiis O, Calabrò R. Right ventricular diastolic dysfunction in arterial systemic hypertension: analysis by pulsed tissue Doppler. *Eur J Echocardiogr* 2002;3:135-142.
19. Galderisi M, Nistri S, Mondillo S, Losi MA, Innelli P, Mele D, Muraru D, D'Andrea A, Ballo P, Sgalambro A, Esposito R, Marti G, Santoro A, Agricola E, Badano LP, Marchioli R, Filardi PP, Mercurio G, Marino PN; Working Group of Echocardiography, Italian Society of Cardiology. Methodological approach for the assessment of ultrasound reproducibility of cardiac structure and function: a proposal of the study group of Echocardiography of the Italian Society of Cardiology (Ultra Cardia SIC) part I. *Cardiovasc Ultrasound* 2011;9:26.
20. Galderisi M, Esposito R, Schiano-Lomoriello V, Santoro A, Ippolito R, Schiattarella P, Strazzullo P, de Simone G. Correlates of global area strain in native hypertensive patients: a three-dimensional speckle-tracking echocardiography study. *Eur Heart J Cardiovasc Imaging* 2012; 13:730-738.

21. Innelli P, Esposito R, Olibet M, Nistri S, Galderisi M. the impact of ageing on right ventricular longitudinal function in healthy subjects: a pulsed Tissue Doppler study. *Eur J Echocardiogr* 2009;10:491-498.
22. Vitale G, Galderisi M, Colao A, Innelli P, Guerra G, Guerra E, Dini FL, Orio F Jr, Soscia A, de Divitiis O, Lombardi G. Circulating IGF-I levels are associated with increased biventricular contractility in top-level rowers. *Clinical Endocrinology* 2008;69:231–236.
23. Grapsa J, Gibbs JS, Dawson D, Watson G, Patni R, Athanasiou T, Punjabi PP, Howard LS, Nihoyannopoulos P. Morphologic and functional remodeling of the right ventricle in pulmonary hypertension by real time three dimensional echocardiography. *Am J Cardiol* 2002;15:906-913.
24. Iriart X, Montaudon M, Lafitte S, Chabaneix J, Réant P, Balbach T, Houle H, Laurent F, Thambo JB. Right ventricle three-dimensional echography in corrected tetralogy of Fallot: accuracy and variability. *Eur J Echocardiogr* 2009;10:784-792.
25. Shiota T. 3D echocardiography: evaluation of the right ventricle. *Curr Opin Cardiol* 2009;24:410–414
26. Johri AM, Passeri JJ, Picard MH. Three dimensional echocardiography: approaches and clinical utility. *Heart* 2010;96:390–397
27. D'Andrea A, Caso P, Bossone E, Scarafile R, Riegler L, Di Salvo G, Gravino R, Cocchia R, Castaldo F, Salerno G, Golia E, Limongelli G, De Corato G, Cuomo S, Pacileo G, Russo MG, Calabrò R. Right ventricular myocardial involvement in either physiological or pathological left ventricular hypertrophy: an ultrasound speckle-tracking two-dimensional strain analysis. *Eur J Echocardiogr.* 2010;11:492-500.

28. Altekin RE, Karakas MS, Yanikoglu A, Ozel D, Ozbudak O, Demir I, Deger N. Determination of right ventricular dysfunction using the speckle tracking echocardiography method in patients with sleeping apnea. *Cardiol J* 2012;19:130-139.
29. Tamborini G, Marsan NA, Gripari P, Maffessanti F, Brusoni D, Muratori M, Caiani EG, Fiorentini C, Pepi M. Reference values for right ventricular volumes and ejection fraction with real-time three-dimensional echocardiography: evaluation in a large series of normal subjects. *J Am Soc Echocardiogr* 2010;23:109-15.
30. Tamborini G, Muratori M, Brusoni D, Celeste F, Maffessanti F, Caiani EG, Alamanni F, Pepi M. Is right ventricular systolic function reduced after cardiac surgery? A two- and three-dimensional echocardiographic study. *Eur J Echocardiogr* 2009;10:630-634.
31. Le Gerche A, Jurcut R, Voigt JU. Right ventricular function by strain echocardiography, *Curr Opin Cardiol* 2010;25:430-436.

Figures

Figure 1. RT3DE study of the right ventricle. 2D RV multiplane display and 3D RV transversal plane during acquisition (upper panel) as well as 9-slice display after acquisition were used for quality check (lower panel).

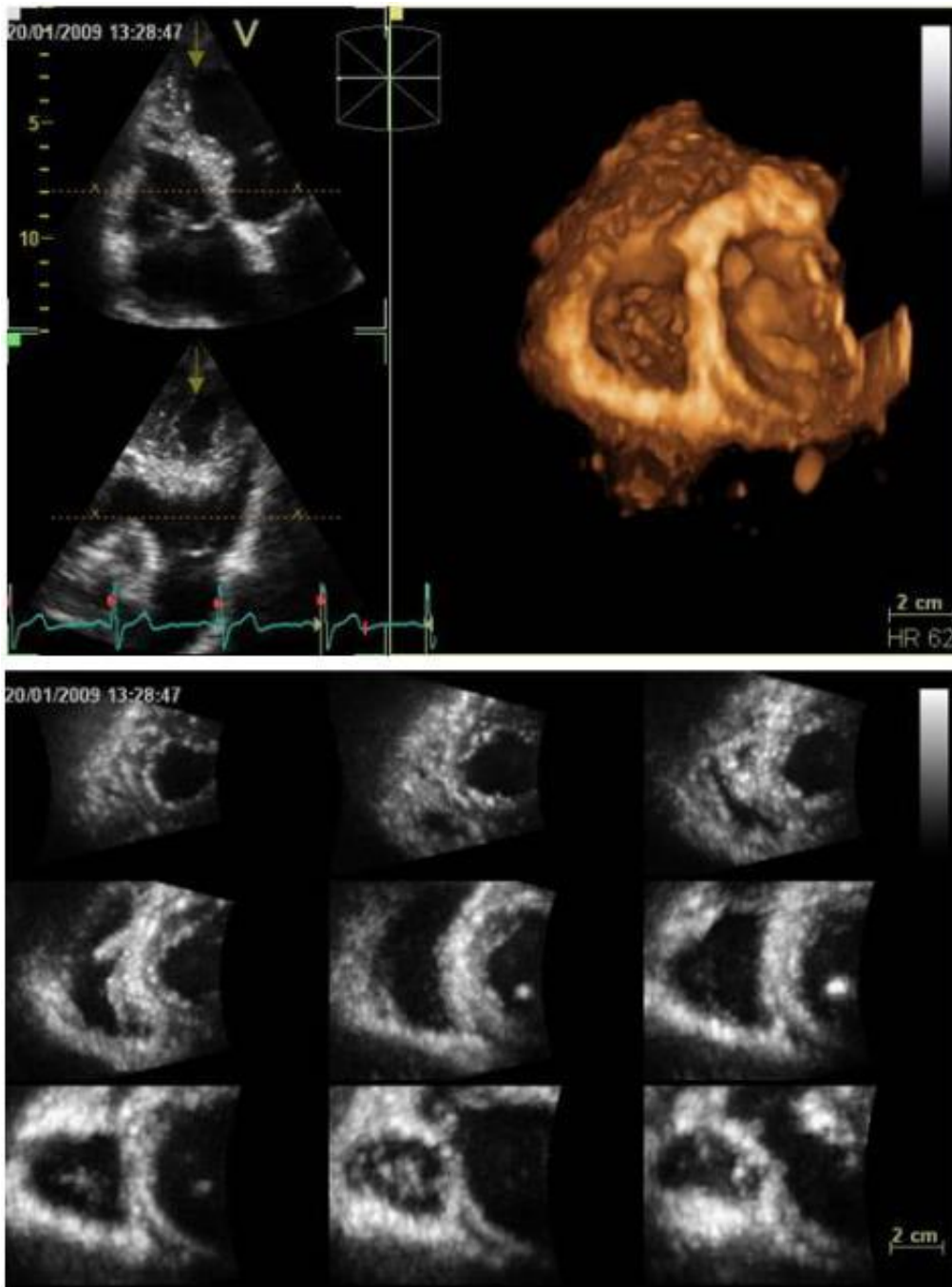


Figure 2. Final determination of RV end-diastolic volume (EDV), end-systolic volume (ESV), ejection fraction (EF) and stroke volume (SV) by RT3DE.

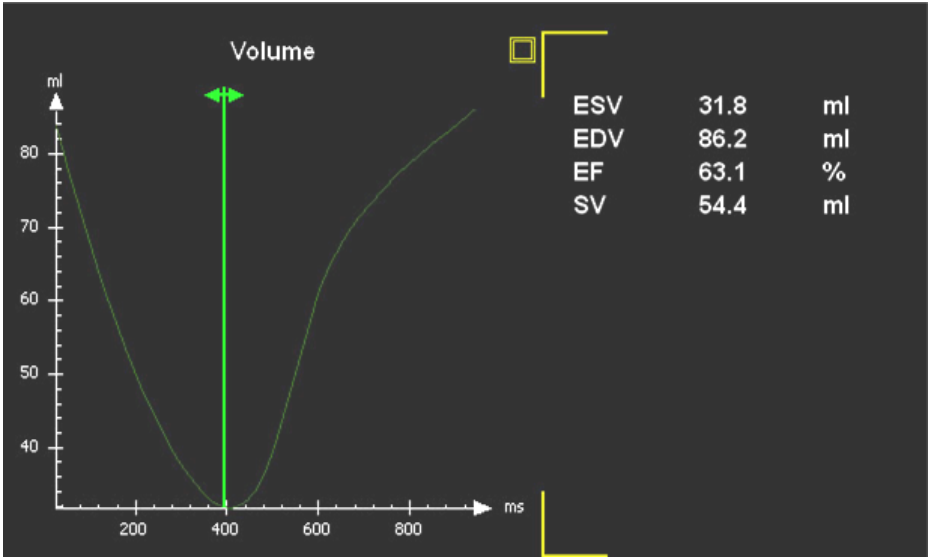
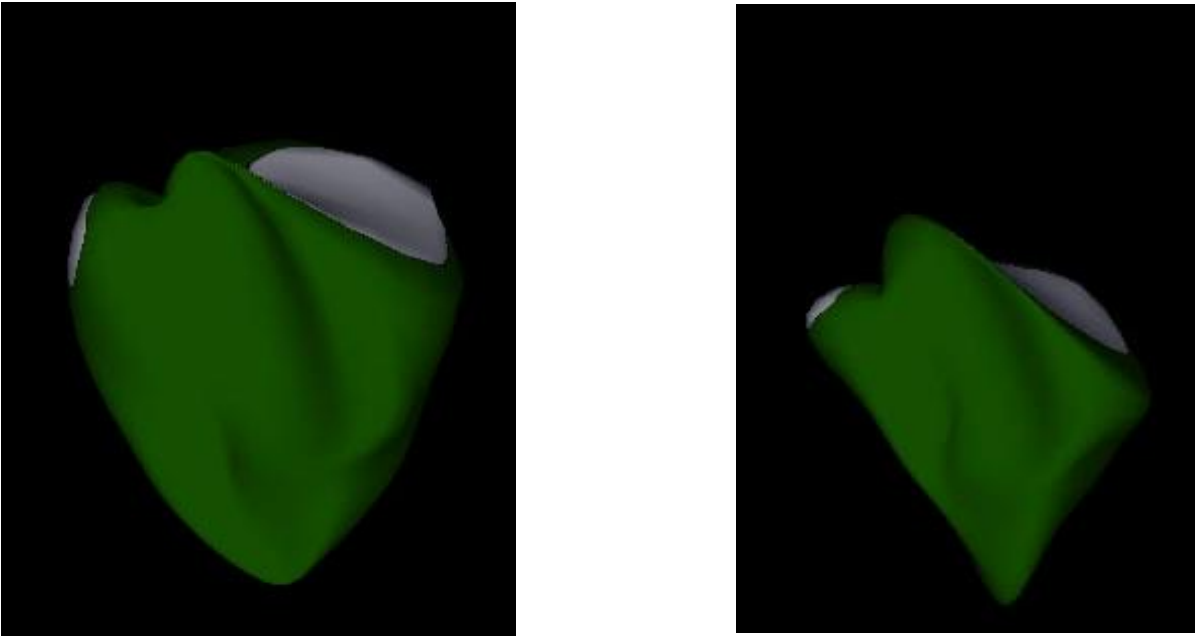


Figure 3. Assessment of RV regional longitudinal function (6 segments, 3 of RV lateral wall and 3 of interventricular septum) by STE. In left upper panel, color representation of each myocardial segment longitudinal strain is superimposed on 2D imaging; in left lower panel, qualitative color M-mode strain representation referring to the 6 consecutive myocardial segments is showed; in right panel, changes in longitudinal strain of each myocardial segment during cardiac cycle is represented by colored curves with dotted white line corresponding to average strain.

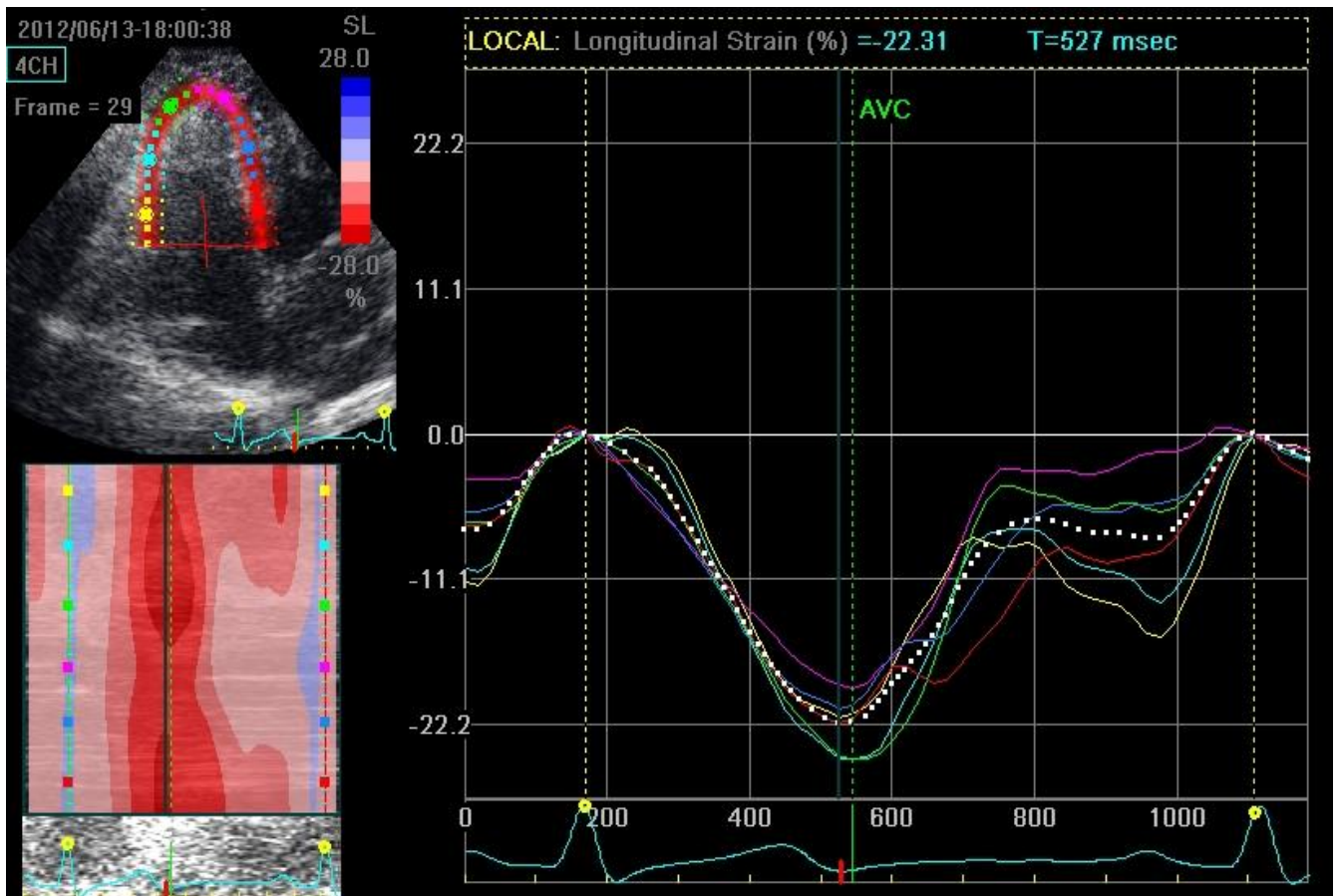


Figure 4. Scatterplot and regression line between RV end-diastolic volume (EDV) (x-line) and RV lateral longitudinal strain (y line) in healthy sedentary controls (green dots) and rowers (blue dots).

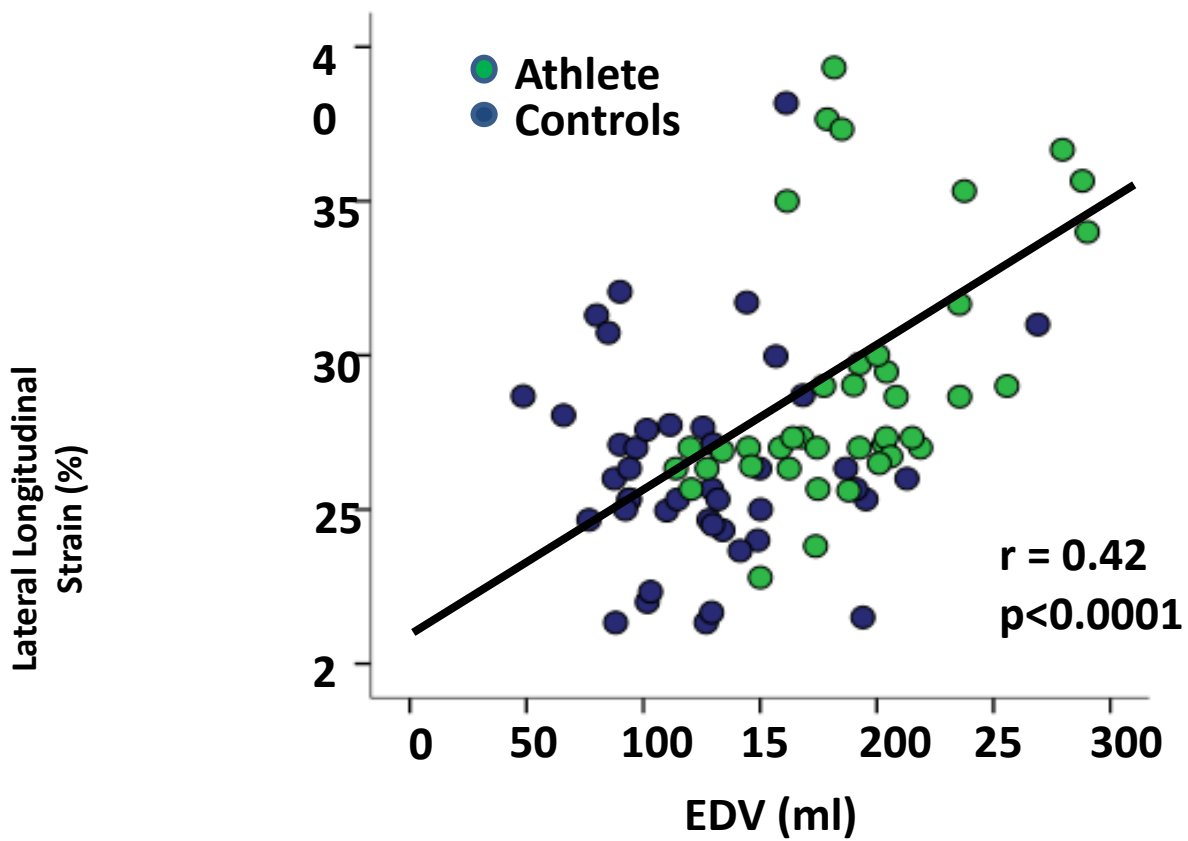
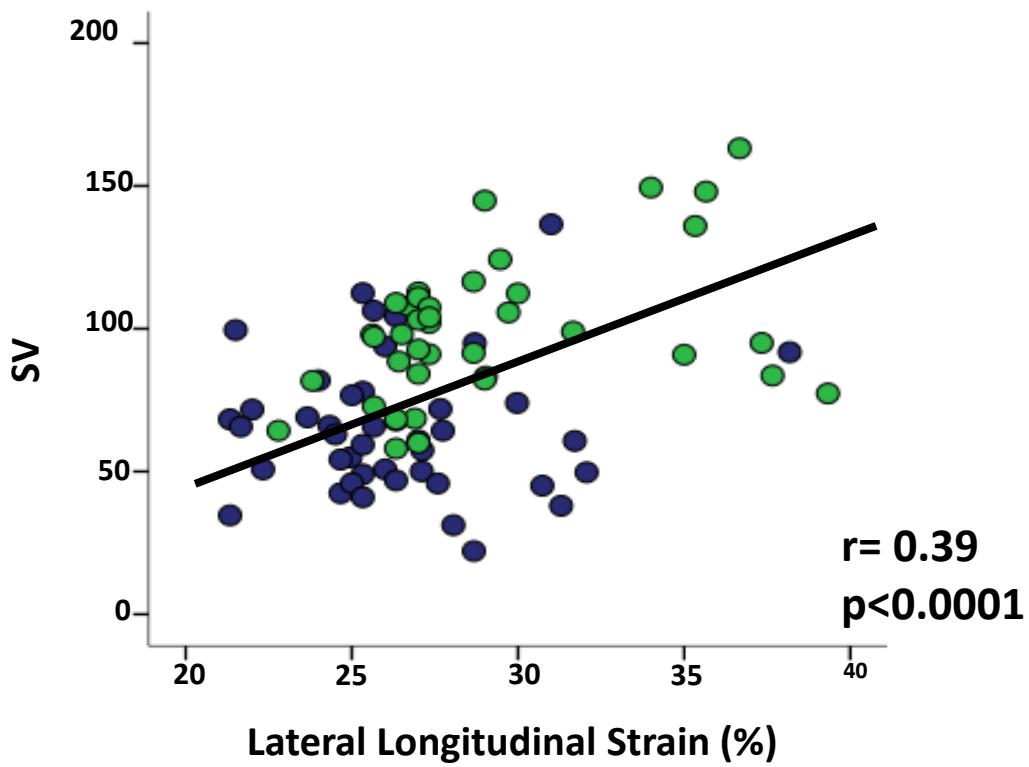


Figure 5. Scatterplot and regression line between RV lateral longitudinal strain (x-line) and RV stroke volume (y-line) in healthy sedentary controls and athletes.



Tables

Table 1: Characteristics of the study population

	Controls (n = 43)	Athletes (n = 40)	p
Age (years)	29.0±5.8	28.3±9.5	ns
BMI (Kg/m²)	23.2±3.0	24.2±2.5	ns
Systolic BP (mmHg)	118.5±11.6	122.4±8.3	ns
Diastolic BP (mmHg)	70.8±8.5	70.9±8.0	ns
Mean BP (mmHg)	86.7±8.1	88.1±7.3	ns
Heart Rate (bpm)	68.4±10.6	55.3±8.0	<0.0001

BMI = Body Mass Index, BP = Blood Pressure

Table 2: Right Ventricular standard Echo Doppler parameters.

	Controls (n = 43)	Athletes (n= 40)	p
RV basal diameter (mm)	27.3±4.9	33.9±5.2	<0.001
RV mid-cavity diameter (mm)	31.4±4.4	38.4±5.2	<0.001
RV longitudinal diameter (mm)	68.0±8.1	75.3±9.4	<0.001
TAPSE (mm)	23.0±3.2	25.6±2.4	<0.001
Tricuspid inflow E/A ratio	1.7±0.4	1.9±0.4	<0.005
Tricuspid annular s' (cm/sec)	0.10±0.02	0.10±0.02	<0.002
Tricuspid annular e' (cm/sec)	0.10±0.02	0.20±0.03	<0.002
Tricuspid annular a' (cm/sec)	0.10±0.04	0.10±0.03	ns
RV E/e' ratio	4.0±0.8	3.8±0.9	ns

RV = Right Ventricle, TAPSE = Tricuspid annular peak systolic excursion

Table 3: RT3DE derived RV parameters.

	Controls (n = 43)	Athletes (n = 40)	p
RV EDV (ml)	127±44	189±44	<0.0001
RV ESV (ml)	61±23	89±24	<0.0001
RV SV(ml)	65±28	100±24	<0.0001
RV EF (%)	52±6	53±6	ns

EF = Ejection Fraction, EDV =End Diastolic Volume, ESV = End Systolic Volume, RV = Right Ventricle

Table 4: STE RV longitudinal strain parameters.

	Controls (n = 43)	Athletes (n = 40)	p
RV GLS (%)	-24±2	-26±3	<0.005
RV LLS (%)	-26±4	-29±4	<0.0001
RV SLS (%)	-23±4	-24±4	Ns

GLS = Global Longitudinal Strain, LLS = Lateral longitudinal strain, SLS = Septal longitudinal strain, RV = Right Ventricular

Table 5: Univariate correlations of STE parameters in pooled population.

Dependent variable	TAPSE	s'	SV(3D)
GLS	r=0.11	r=0,20	r=0.20
	Ns	ns	Ns
LLS	r=0.19	r=0.15	r=0.99
	Ns	ns	p<0.0001
SLS	r=0.06	r=0.12	r=0.06
	Ns	ns	Ns

Second Study: Background

Using new echocardiographic technologies, especially Speckle Tracking Echocardiography, we developed the second study accepted for publication on Hypertension. We evaluated impact of pulse pressure on left ventricular systolic function. We enrolled 143 patients (68 newly hypertensive patients, never treated, and 75 normotensive subjects), all patients underwent complete echocardiographic study, with Doppler and Spckle Tracking. Study population was divided in two groups according pulse pressure tertiles. Group 1 included the first and the second tertile (n = 93 with pulse pressure < 55mmHg), group 2 included the third tertile (n = 50 with pulse pressure > 55mmHg). Left ventricular mass was significantly higher in the third pulse pressure tertile, while relative wall thickness did not significantly differ. Global longitudinal strain and E/A ratio were lower in the third tertile, while E/e' ratio resulted higher. Moreover multiple linear regression analysis showed that pulse pressure and overweight were independently correlated to global longitudinal strain. Thus, elevated pulse pressure negatively impacts on left ventricular longitudinal function.

Second Study:

Impact of pulse pressure on left ventricular global longitudinal strain in normotensive and newly diagnosed, untreated hypertensive patients

Abstract

Objectives: Little is known about the impact of pulse pressure (PP) on left ventricular (LV) systolic function. Aim of our study was to evaluate whether high PP is associated with subclinical

28

LV systolic dysfunction.

Methods: The study population included 143 participants (68 newly-diagnosed, never-treated hypertensive and 75 normotensive subjects) evaluated by echo-Doppler, including determination of global longitudinal strain (GLS) by Speckle Tracking. According to PP tertiles, participants were divided in 2 groups: the first group merging the 1st and 2nd PP tertiles (n=93, PP ≤ 55 mmHg) and the second group including the highest PP tertile (HPPT) (n=50, PP > 55 mmHg).

Results: The two groups were comparable for sex, body mass index and heart rate whereas age was higher in subjects with the HPT (p<0.0001). LV mass index was significantly higher in subjects with the HPPT (p<0.01), with no significant difference in relative wall thickness. Among several indices of LV systolic function, only GLS was lower in subjects with the HPPT (p<0.001). Transmitral E/A ratio (p=0.006) was lower and E/e' ratio higher (p<0.001) in the HPPT group. By a multilinear regression analysis, HPPT (p<0.020) and overweight (p=0.025) were independent correlates of low GLS. Replacing HPPT with the highest systolic blood pressure (SBP) tertile, GLS was independently associated with body mass index (p=0.040) but not with the highest SBP tertile (p=0.069). **Conclusion:** Elevated PP negatively influences LV longitudinal mechanics in a mixed population of normotensive and untreated hypertensive subjects.

Introduction

Recent ESC/ESH guidelines for management of arterial hypertension consider the absolute values of systolic and/or diastolic blood pressure (BP) to classify hypertensive stages and cardiovascular (CV) risk [1]. However, another important feature taken into account is pulse pressure (PP), which is calculated as the difference between systolic and diastolic BP. PP exhibits a wide range of values, depending on increased systolic BP, decreased diastolic BP or both [2]. PP is a raw estimate of arterial stiffness [3-6] and is directly related to CV alterations found in hypertensive

patients [7-10]. Although CV remodeling and dysfunction are mainly due to the mechanical stress resulting from elevated systolic and/or diastolic BP [11-12], PP is critically important as the pressure amplification of LV stroke at the level of conduit arteries [12,13]. PP has been demonstrated to increase CV risk in middle-aged [2,14] and elderly subjects [15]. It was also independently associated with subclinical CV disease in the 6776 participants of the Multiethnic Study of Atherosclerosis, which included both normotensive and hypertensive patients [16]. In this view, it is conceivable that PP could be considered a marker of pre-clinical CV disease rather than a true CV risk factor [17].

Speckle Tracking Echocardiography (STE), a simple and feasible ultrasound technique which can be easily performed during a standard echocardiographic exam, provides a quantitative analysis of LV deformation in the three orthogonal planes (longitudinal, circumferential and radial) and LV twisting [18-20]. Among the different LV deformation components, global longitudinal strain (GLS) has been identified to be an earlier marker of subclinical cardiac damage than LV ejection fraction [18-20]. Worthy of note, reduced GLS has also been found to be associated with a two-element windkessel model estimate of arterial stiffness (PP/stroke volume ratio) in a middle age series, which included 70 hypertensive patients and 30 normotensive volunteers [21].

The present study was designed to evaluate the relation between PP and LV systolic function in a population of normotensive and untreated hypertensive subjects, by assessing several echocardiographic systolic indices - including GLS – in relation with the other BP components, LV geometry and parameters of diastolic function.

Methods

Study population

After their informed consent was obtained, 68 consecutive, newly-diagnosed, never-treated

hypertensive outpatients and 75 normotensive subjects, recruited among the staff of the Federico II University hospital on a voluntary basis for a screening on early diagnosis of hypertension, underwent a standard transthoracic echo-Doppler study, including STE of the three apical views. Criteria of exclusion were age < 30 years, diabetes mellitus, coronary artery disease, overt heart failure, valve heart disease (any stenosis and more than trivial mitral or aortic regurgitation), primary cardiomyopathies, atrial fibrillation or inadequate echocardiographic imaging. The diagnosis of arterial hypertension was established for BP values \geq 140 mmHg systolic and/or 90 diastolic BP as the average of three measurements in the sitting position in three different visits. BP was also measured in supine position by a cuff sphygmomanometer at the end of echocardiographic exam (average of three measurements) and this measurement was chosen for statistical analysis in order to obtain an almost simultaneous evaluation of echocardiographic parameters and LV afterload.

Echo Doppler examination

Standard echo Doppler and STE were performed by a Vivid E9 ultrasound machine (GE Healthcare, Horten, Norway), using a 2.5 MHz transducer with harmonic capability.

Two-dimensional and Doppler exam were performed according to the standards of our laboratory [22,23]. The quantitative analysis of the left ventricle was done in agreement of 2015 ASE/EACVI recommendations [24]. Two-dimensional echocardiographic LV ejection fraction was computed from LV end-diastolic and end-systolic volumes (from apical 4- and 2-chamber views) measured by the modified Simpson rule. LV mass was calculated by 2D guided M-mode imaging or directly from 2D longitudinal long-axis view and indexed for height powered to 2.7 [25]. LV hypertrophy was defined as LV mass index $> 47 \text{ g/m}^{2.7}$ in women and $> 50 \text{ g/m}^{2.7}$ in men [26].

Relative diastolic wall thickness was computed as the sum of anterior septal wall thickness and posterior wall thickness divided by LV diastolic diameter. Midwall fractional shortening was

31

calculated according to a validated formula as an index of LV midwall mechanics [27]. Left atrial volume (area-length method in apical 4- and 2-chamber views) was indexed for body surface area [24]. Transmitral Doppler inflow and pulsed Tissue Doppler were recorded in apical 4-chamber view. The average of the peak early systolic (s') and diastolic velocity (e') of the septal and lateral mitral annulus velocities were calculated and the ratio of transmitral peak early velocity (E) to average e' (E/ e' ratio) derived as an estimate of LV filling pressure [22,23,28]. All Doppler measurements were averaged from 3 cardiac cycles.

STE procedures were performed according to the standard of our laboratory [23]. STE of the left ventricle was recorded on 2-D images of three consecutive cardiac cycles from the three apical views (long axis, 4- and 2-chamber) at an approximately equal heart rate. LV cavity was recorded with the narrowest scan and at the lowest possible depth in order to obtain the left ventricle as large as possible on the screen and a frame rate of 40-70 frames/s. The same field depth was maintained for all the views. An interactive software (endocardial-cavity interface traced manually and epicardial tracing generated automatically) rejects segments of poor imaging quality, allowing the observer to manual override its decision by visual assessment. The time of aortic valve closure (AVC) was marked in the apical long-axis view, as the driving view, and used as reference point in all the other views. Each of the three apical images was automatically divided into 6 myocardial segments. Peak negative longitudinal strain was measured from 6 segments in each of the 3 apical views (long-axis, 4- and 2-chamber) and global longitudinal strain (GLS) calculated as the average of individual percent peak strain before AVC. Reproducibility of STE in our laboratory has been previously reported [29].

Statistical analysis

Statistical analysis was performed by SPSS package, release 12 (SPSS Inc, Chicago, Illinois, USA). Data are presented as mean value \pm SD. Participants were divided into tertiles of PP, and

the highest tertile was compared to the merged lowest and middle tertiles. The cut point of the highest tertile (i.e. the 67th percentile of the distribution) was ≥ 55 mmHg. Descriptive statistics was obtained by one-factor ANOVA/ANCOVA and χ^2 distribution with computation of exact p value by Monte Carlo method. Least squares linear regression was used to evaluate univariate correlates of a given variable. Multiple linear regression analyses were performed to study independent correlates of GLS, also considering potential multicollinearity by computation of variance inflation factor. Collinearity was considered acceptable and regression model stable for variance inflation factor <3 . The null hypothesis was rejected at 2-tailed $p < 0.05$.

Results

The HPPT included 50 subjects while the other group (1st and 2nd tertile) comprised together 93 subjects. In the HPPT, 33 (66.0%) were hypertensive and 17 (34%) were normotensive.

The clinical characteristics of the two study groups are listed in **Table 1**. The two groups were comparable for sex-distribution, body mass index, heart rate and diastolic BP. Systolic BP, mean BP (both $p < 0.0001$) and age ($p < 0.0001$) were higher in the HPPT.

Table 2 shows that LV mass index ($p < 0.01$) was higher in the HPPT than in the other group, without significant differences in relative wall thickness. Among the different indices of LV systolic function, only GLS was significantly lower in the HPPT ($p < 0.001$). By restricting the analysis to the hypertensive group, GLS was confirmed lower in the HPPT (-19.2 ± 1.9 vs. $-20.4 \pm 2.2\%$, $p < 0.02$).

Among LV diastolic parameters, transmitral E/A ratio ($p = 0.006$) and e' velocity ($p < 0.0001$) were lower in the HPPT, whereas a' velocity ($p < 0.005$) and E/e' ratio ($p < 0.001$) were higher.

LV hypertrophy was detected in 8/143 (5.6%, all in the hypertensive group) of the study population, 6/50 patients in the HPPT (12.0%) and 2/75 in the other group (2.7%) ($p < 0.01$).

Univariate correlations

Table 3a shows the univariate relations of GLS and PP in the pooled population. GLS was negatively correlated to body mass index, systolic BP, diastolic BP, mean BP and PP (**Figure 1**). PP was positively related to age, LV mass index and E/e' ratio and negatively to average e' (**Table 3b**). Even after adjusting for age, sex and mean BP (ANCOVA), the correlation between GLS and PP remained significant ($p=0.003$; data not in table).

Multiple linear regression analyses

By a multiple linear regression analysis - including age, body mass index, HPPT, LV mass index and E/e' ratio as potential independent correlates of GLS in the whole population - HPPT ($p<0.020$) and overweight ($p<0.025$) were independently associated with the lowest GLS, with PP exhibiting the highest standardized β -coefficient (**Table 4**, Model 1). Replacing HPPT with the highest systolic BP tertile (≥ 140 mmHg), GLS was independently associated with body mass index ($p=0.040$) but not with the highest systolic BP tertile ($p=0.069$) (**Table 4**, Model 2). In a subsequent multiple linear regression analysis we considered age, body mass index, LV mass index and E/e' ratio and both the physiological components of BP, mean BP (as the steady component) and PP (as the pulsatile component). By this analysis, GLS was independently associated with PP (standardized β coefficient = -0.204 , $p=0.031$) and body mass index ($\beta = -0.181$, $p=0.040$,) but not with mean BP ($\beta = -0.133$, $p=0.191$) (cumulative $R^2= 0.11$, $SEE = 2.4\%$, $p<0.01$) (data not shown in Table 4).

Discussion

Our findings demonstrate that in a population which included both normotensive and hypertensive subjects (1) GLS is significantly lower in the HPPT corresponding to abnormally increased PP (≥ 55 mmHg) and (2) GLS and elevated PP are associated independently of clinical and

echocardiographic confounders. In this context, high PP - corresponding to the 67th percentile of the distribution - has the strongest impact on GLS.

Arterial stiffness is a predictor of cardiovascular morbidity and mortality [30]. Increased PP is generally accepted as a raw index of arterial stiffness and a marker of arteriosclerosis, as it reflects the difficulty in distending conduit arteries and the loss of arterial elasticity [3-6]. Thus, PP could be considered as an independent marker of established pre-clinical CV disease more than a true CV risk factor [17].

In the present study we chose the third PP tertile (HPPT = $PP \geq 55$ mmHg) as representative of abnormally increased PP. It is of interest that a definite cut-off point of 55 mmHg for normal PP, was reported also as the highest percentile of the distribution in the normal population of the Reference Values for Arterial Measurements Collaboration Group [31]. The choice of this cut-off point, lower than that reported in other studies [16,17], can be further justified by the fact that our population comprised normotensive and newly diagnosed hypertensive subjects, with a low prevalence of LV hypertrophy (= 5.6%), a finding which can be explained with the likely short duration of elevated BP history. Nevertheless, GLS was significantly reduced in subjects with high PP and this difference remained significant even when tested in the only hypertensive patients.

Previous studies investigated possible association of both arterial stiffness and PP with LV diastolic dysfunction in hypertensive patients [32,33]. In particular, Mottram et al observed an independent association between PP and the degree of E/e' ratio, taken as a non-invasive estimate of LV filling pressure [32]. Our study is the first to extend the association of PP with a parameter of LV systolic function. We explored not only GLS but also other indices of LV systolic function: an index of LV chamber function such as ejection fraction, an estimate of wall mechanics such as midwall fractional shortening, prognostically validated in arterial

hypertension [26], and a good surrogate of LV longitudinal function of LV base as s' velocity of mitral annulus is [18]. Among these LV systolic indices, only GLS was able to differentiate subjects with normal and elevated PP.

GLS refers to LV longitudinal function and is thought to be due to the shortening of cardiomyocytes that are longitudinally oriented in subendocardium [18-20]. It has been shown to be a much more precocious index of LV longitudinal dysfunction than s' velocity [18]. GLS has been studied in several cardiac conditions, and it was always able to detect early subclinical dysfunction [18-20]. GLS has been also demonstrated to be a prognosticator in the clinical setting [34].

Univariate relations provided additional information in the present study as they highlighted an inverse association between PP and GLS considered as continuous variables (both in the pooled population and in hypertensive group). The choice of potential confounders in the multivariate analyses involved age, body mass index, diastolic BP, LV mass, E/e' ratio because of their relationships with GLS and or PP [18-20,35,36]. After adjusting for these confounders, the HPPT, i.e. an abnormally elevated PP, and GLS remained independently associated in the pooled population. Conversely, if we considered the highest systolic BP tertile, it did not enter the model in alternative analysis. We could not test simultaneously PP and systolic BP because of their high level of collinearity. Thus, we may speculate that the association of elevated PP with GLS reduction is not simply due to the elevated systolic BP. Systolic BP, representing the peak of BP change, is essential for PP trait but it is not the only determinant. To better understand pathophysiology of GLS, we also compared the independent associations of two hemodynamic components of pressure and flow: mean BP, which represents the steady component and the same PP, i.e. the pulsatile component [37]. Both factors contribute to the mechanisms underlying arterial hypertension but, in the present study, only PP was related to the very precocious LV systolic

impairment expressed by a lower GLS.

To the best of our knowledge, our study is the first one demonstrating a correlation between PP and early LV systolic dysfunction in a population including both hypertensive patients and healthy normotensive. The increase of BP is a gradual process and the CARDIA study [38] has very recently shown that, over the years, cumulative BP (millimeters of mercury x year) exerts a negative impact on GLS (but not on ejection fraction). In the CARDIA study, though few subjects exceeded thresholds for BP treatment, LV dysfunction associated with cumulative BP was unrelated to a specific BP threshold, which reflects the uncertainty in establishing a definite cut-off value for deciding BP treatment.

Increased PP is clearly associated with cardiovascular remodeling, involving both vessels and heart. Development of sclerosis in arteries is responsible of the arterial stiffness while an early development of myocardial fibrosis is responsible of the negative influence on LV longitudinal function. Myocardial fibrosis has been shown to be associated with increased arterial stiffness [39] and LV longitudinal dysfunction [40]. We recently demonstrated that in uncomplicated hypertensive patients the presence of myocardial fibrosis detected by late gadolinium enhancement applied to cardiac magnetic resonance is independently associated with a lower GLS [41]. Longitudinal strain and torsion have been found also to correlate significantly with serum levels of tissue inhibitor of matrix metalloproteases, a marker of myocardial interstitial fibrosis, in hypertensive patients [42]. Our data also confirm previous studies reporting a reduction of GLS in young hypertensives [29] and in borderline pre-hypertensive subjects [43], two categories of subjects in which the cardiac damage is believed to be minimal or even absent.

In conclusion, our study confirms the role of PP as a pre-clinical marker of target organ damage extending its negative impact on LV longitudinal function, when other indices of LV systolic function are still normal, in a population of both normotensive and hypertensive subjects. This

association is independent of major confounders, such as overweight, LV hypertrophy, and LV diastolic dysfunction. Subjects with abnormally clinical high PP could be therefore identified as a group at risk for development of subsequent heart failure. In this clinical setting assessment of LV longitudinal function might be worth to identify very early myocardial dysfunction.

References

1. Mancia G, Fagard R, Narkiewicz K, Redon J, Zanchetti A, Böhm M, et al. 2013 ESH/ESC guidelines for the management of arterial hypertension: the Task Force for the Management of Arterial Hypertension of the European Society of Hypertension (ESH) and of the European Society of Cardiology (ESC). *J Hypertens* 2013;31:1281-1357.
2. Franklin SS, Khan SA, Wong ND, Larson MG, Levy D. Is pulse pressure useful in predicting risk for coronary heart disease? The Framingham heart study. *Circulation* 1999;100:354-360.
3. Girerd X, Laurent S, Pannier B, Asmar R, Safar M. Arterial distensibility and left ventricular hypertrophy in patients with sustained essential hypertension. *Am Heart J* 1991;122:1210– 1214.
4. Chugh A, Bakris GL. Pulse pressure and arterial stiffness: an emerging renal risk predictor? *J Hypertens* 2007 Sep;25(9):1796-7.
5. Safar M, London G, Asmar R, Frohlich E. Recent advances on large arteries in hypertension. *Hypertension* 1998;32:156–161.
6. Safar ME. Systolic blood pressure, pulse pressure and arterial stiffness as cardiovascular risk factors. *Curr Opin Nephrol Hypertens* 2001;10:257–261.
7. Safar ME, Nilsson PM, Blacher J, Mimran A. Pulse Pressure, arterial stiffness, and end-organ damage. *Curr Hypertens Rep* 2012;14:339–344.

8. Safar ME. Pulse pressure in essential hypertension: clinical and therapeutic implications. *J Hypertens* 1989;7:769-776.
9. Roman M, Ganau A, Saba P, Pini R, Pickering T, Devereux R. Impact of arterial stiffening on left ventricular structure. *Hypertension* 2000;36:489-494.
10. Kawaguchi M, Hay I, Fetters B, Kass D. Combined ventricular systolic and arterial stiffening in patients with heart failure and preserved ejection fraction: implications for systolic and diastolic reserve limitations. *Circulation* 2003;107:714-720.
11. Zheng M, Xu X, Wang X, Huo Y, Xu X, Qin X, et al. Age, arterial stiffness, and components of blood pressure in Chinese adults. *Medicine* 2014;93:e262..
12. de Simone G, McClelland R, Gottdiener JS, Celentano A, Kronmal RA, Gardin JM. Relation of hemodynamics and risk factors to ventricular-vascular interactions in the elderly: the Cardiovascular Health Study. *J Hypertens* 2001;19:1893-1903.
13. Viazzi F, Leoncini G, Parodi D, Ravera M, Ratto E, Vettoretti S, et al. Pulse pressure and subclinical cardiovascular damage in primary hypertension. *Nephrol Dial Transplant* 2002;17:1779-1785.
14. Haider AW, Larson MG, Franklin SS, Levy D; Framingham Heart Study. Systolic blood pressure, diastolic blood pressure, and pulse pressure as predictors of risk for congestive heart failure in the Framingham Heart Study. *Ann Intern Med* 2003;138:10-16.
15. Benetos A, Safar M, Rudnicki A, Smulyan H, Richard JL, Ducimetiere P, Guize L. Pulse pressure: a predictor of long-term cardiovascular mortality in a French male population. *Hypertension* 1997;30:1410-1415.
16. Winston GJ, Palmas W, Lima J, Polak JF, Bertoni AG, Burke G, et al. Pulse pressure and subclinical cardiovascular disease in the Multi-Ethnic Study of Atherosclerosis. *Am J Hypertens* 2013;26:636-642.

17. de Simone G, Roman MJ, Alderman MH, Galderisi M, de Divitiis O, Devereux RB. Is high pulse pressure a marker of preclinical cardiovascular disease? *Hypertension* 2005;45:575-579.
18. Mor-Avi V, Lang RM, Badano LP, Belohlavek M, Cardim NM, Derumeaux G, Galderisi M, et al. Current and evolving echocardiographic techniques for the quantitative evaluation of cardiac mechanics: ASE/EAE consensus statement on methodology and indications endorsed by the Japanese Society of Echocardiography. *Eur J Echocardiogr* 2011;12:167-205.
19. Mondillo S, Galderisi M, Mele D, Cameli M, Lomoriello VS, Zacà V, et al. (Echocardiography Study Group of the Italian Society of Cardiology). Speckle-tracking echocardiography: a new technique for assessing myocardial function. *J Ultrasound Med* 2011;30:71-83
20. Geyer H, Caracciolo G, Abe H, Wilansky S, Carerj S, Gentile F, et al. Assessment of myocardial mechanics using speckle tracking echocardiography: fundamentals and clinical applications. *J Am Soc Echocardiogr* 2010; 23:351–369.
21. Pavlopoulos H, Nihoyannopoulos P. Pulse pressure/stroke volume: a surrogate index of arterial stiffness and the relation to segmental relaxation and longitudinal systolic deformation in hypertensive disease. *Eur J Echocardiogr* 2009;10:519–526.
22. Innelli P, Sanchez R, Marra F, Esposito R, Galderisi M. The impact of aging on left ventricular longitudinal function in healthy subjects: a pulsed tissue Doppler study. *Eur J Echocardiogr* 2008;9:241-249.
23. Galderisi M, Nistri S, Mondillo S, Losi MA, Innelli P, Mele D, Muraru D, et al. Working Group of Echocardiography, Italian Society of Cardiology. Methodological approach for the assessment of ultrasound reproducibility of cardiac structure and function: a proposal of the

study group of Echocardiography of the Italian Society of Cardiology (Ultra Cardia SIC) part

I. *Cardiovasc Ultrasound* 2011 Sep 26;9:26.

24. Lang RM, Badano LP, Mor-Avi V, Afilalo J, Armstrong A, Ernande L, et al. Recommendations for cardiac chamber quantification by echocardiography in adults: an update from the American Society of Echocardiography and the European Association of Cardiovascular Imaging. *Eur Heart J Cardiovasc Imaging* 2015;15:233-270.
25. de Simone G, Kizer JR, Chinali M, Roman MJ, Bella JN, Best LG, et al; Strong Heart Study Investigators. Normalization for body size and population-attributable risk of left ventricular hypertrophy: the Strong Heart Study. *Am J Hypertens* 2005;18:191-196.
26. de Simone G, Daniels SR, Devereux RB, Meyer RA, Roman MJ, de Divitiis O, Alderman MH. Left ventricular mass and body size in normotensive children and adults: assessment of allometric relations and impact of overweight. *J Am Coll Cardiol* 1992;20:251-260.
27. de Simone G, Devereux RB, Koren MJ, Mensah GA, Casale PN, Laragh JH. Midwall left ventricular mechanics. An independent predictor of cardiovascular risk in arterial hypertension. *Circulation* 1996;93:259-265.
28. Nagueh SF, Appleton CP, Gillebert TC, Marino PN, Oh JK, Smiseth OA, et al. Recommendations for the evaluation of left ventricular diastolic function by echocardiography. *J Am Soc Echocardiogr* 2009;22:107-133.
29. Galderisi M, Lomoriello VS, Santoro A, Esposito R, Olibet M, Raia R, et al. Differences of myocardial systolic deformation and correlates of diastolic function in competitive rowers and young hypertensives: a speckle-tracking echocardiography study. *J Am Soc Echocardiogr* 2010;23:1190-1198.
30. Laurent S, Boutouyrie P, Asmar R, Gautier I, Laloux B, Guize L, Ducimetiere P, Benetos A. Aortic stiffness is an independent predictor of all-cause and cardiovascular mortality in

hypertensive patients. *Hypertension* 2001;37:1236–1241.

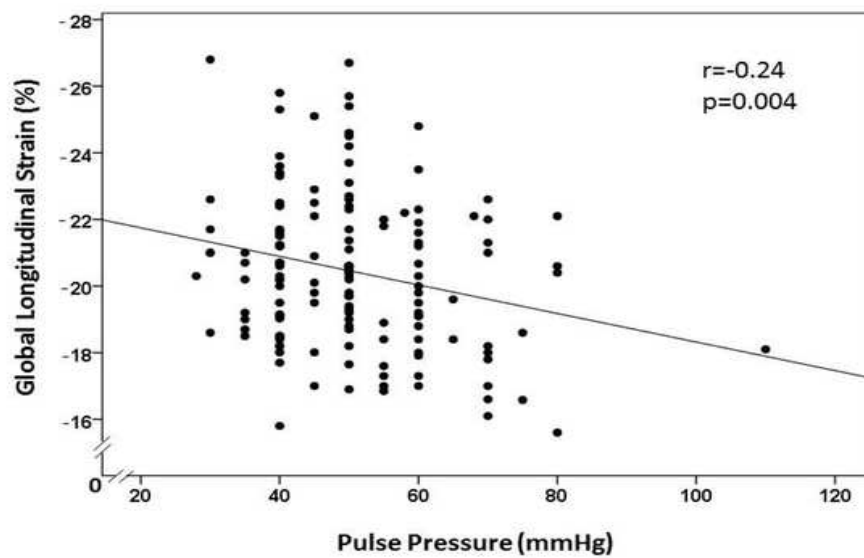
31. Herbert A, Cruickshank JK, Laurent S, Boutouyrie P. Establishing reference values for central blood pressure and its amplification in a general healthy population and according to cardiovascular risk factors. *Eur Heart J* 2014;35:3122–3132.
32. Mottram PM, Haluska BA, Leano R, Carlier S, Case C, Marwick TH. Relation of arterial stiffness to diastolic dysfunction in hypertensive heart disease. *Heart* 2005;91:1551–1556.
33. Zito C, Mohammed M, Todaro MC, Khandheria BK, Cusmà-Piccione M, Oreto G, et al. Interplay between arterial stiffness and diastolic function: a marker of ventricular-vascular coupling. *J Cardiovasc Med* 2014;15:788-796.
34. Kalam K, Otahal P, Marwick TH. Prognostic implications of global LV dysfunction: a systematic review and meta-analysis of global longitudinal strain and ejection fraction. *Heart* 2014;100:1673-1680.
35. Wang YC, Liang CS, Gopal DM, Ayalon N, Donohue C, Santhanakrishnan R, et al. Preclinical systolic and diastolic dysfunction in metabolically healthy and unhealthy obese Individuals. *Circ Heart Fail* 2015 Jul 14 pii: CIRCHEARTFAILURE.114.002026 [Epub ahead of print].
36. Orhan AL, Uslu N, Dayi SU, Nurkalem Z, Uzun F, Erer HB, et al. Effects of isolated obesity on left and right ventricular function: a tissue Doppler and strain rate imaging study. *Echocardiography* 2010;27:236–243.
37. Nichols WW, O'Rourke MF. McDonald's Blood flow in arteries. Theoretical, experimental and Clinical Principles, 4th edn. Edward Arnold: London, 2006; 49–94, 193–233, 339–402, 435–502.
38. Kishi S, Teixido-Tura G, Ning H, Venkatesh BA, Wu C, Almeida A, et al. Cumulative blood pressure in early adulthood and cardiac dysfunction in middle age. The CARDIA

Study. *J Am Coll Cardiol* 2015;65:2679-2687.

39. Puntmann VO, Arroyo Ucar E, Hinojar Baydes R, Ngah NB, Kuo YS, Dabir D, et al. Aortic stiffness and interstitial myocardial fibrosis by native T1 are independently associated with left ventricular remodeling in patients with dilated cardiomyopathy. *Hypertension* 2014;64:762- 768.
40. Ishizu T, Seo Y, Kameda Y, Kawamura R, Kimura T, Shimojo N, Xu D, Murakoshi N, Aonuma K. Left ventricular strain and transmural distribution of structural remodeling in hypertensive heart disease. *Hypertension* 2014;63:500-506.
41. Contaldi C, Imbriaco M, Alcidi G, Ponsiglione A, Santoro C, Puglia M, et al. Assessment of the relationships between left ventricular filling pressures and longitudinal dysfunction with myocardial fibrosis in uncomplicated hypertensive patients. *In J Cardiol* 2016;202:84–86
42. Kang SJ, Lim HS, Choi BJ, Choi SY, Hwang GS, Yoon MH, Tahk SJ, Shin JH. Longitudinal strain and torsion assessed by two-dimensional speckle tracking correlate with the serum level of tissue inhibitor of matrix metalloproteinase-1, a marker of myocardial fibrosis, in patients with hypertension. *J Am Soc Echocardiogr* 2008;21:907-911.
43. Di Bello V, Talini E, Dell'Omo G, Giannini C, Delle Donne MG, Canale ML, et al. Early left ventricular mechanics abnormalities in pre-hypertension: a two-dimensional strain echocardiography study. *Am J Hypertens* 2010;23:405-412.

Figures

Figure 1. Scatterplot and regression line of individual values of pulse pressure (x-line) and corresponding values of GLS (y line) in the pooled population. Values of GLS considered as “positive” (sign +) to build the association in order to homogenize the results of analyses and strengthen their clinical meaning: the higher values the better strain deformation independent on the plus/minus sign.



Tables

Table 1. Clinical data of the study population

	PP <55mmHg (n = 93)	PP ≥ 55 mmHg (n = 55)	P value
Sex (F/M)	40/53	19/31	0.364
Age (years)	45.0 ± 10.7	54.4 ± 11.7	0.0001
BMI (kg/m²)	25.8 ± 3.9	26.6 ± 4.1	0.245
Systolic BP (mmHg)	126.1 ± 12.5	150.8 ± 18.8	0.0001
Diastolic BP (mmHg)	82.8 ± 12.4	86.1 ± 12.8	0.142
Mean BP (mmHg)	97.3 ± 12.1	107.7 ± 14.3	0.0001
Heart rate (bpm)	69.1 ± 13.0	73.7 ± 13.9	0.072

BMI= Body mass index, BP= Blood pressure, PP= pulse pressure

Table 2. Echo-Doppler data of the study population

	PP<55mmHg (n=93)	PP≥55mmHg g (n=50)	P value
IVST (mm)	8.4 ± 1.3	8.8 ± 1.7	0.108
PWT (mm)	8.1 ± 1.2	8.4 ± 1.4	0.176
LVIDd (mm)	49.2 ± 4.7	49.4 ± 5.1	0.785
LVIDs (mm)	32.4 ± 4.4	31.8 ± 6.3	0.572
LVMi (g/m^{2.7})	33.1 ± 6.7	36.6 ± 9.2	0.011
RWTd	0.34 ± 0.05	0.35 ± 0.06	0.165
LVEF (%)	62.7 ± 5.4	62.7 ± 5.9	0.984
MFS (%)	18.0 ± 3.1	17.9 ± 3.1	0.994
Average s' (cm/sec)	9.5 ± 5.0	8.5 ± 1.8	0.159
GLS (%)	-20.9 ± 2.3	-19.5 ± 2.1	0.001
LAV i (ml/m²)	23.4 ± 7.9	26.6 ± 7.9	0.050
E/A ratio	1.21 ± 0.3	0.98 ± 0.3	0.006
DT (ms)	182.5 ± 48.9	208.6 ± 46.5	0.050
Average e' (cm/sec)	11.4 ± 2.8	9.6 ± 2.7	0.0001
Average a' (cm/sec)	10.4 ± 2.0	11.2 ± 2.7	0.005
E/e' ratio	6.63 ± 1.73	7.75 ± 2.39	0.001

DT= E velocity deceleration time, GLS= Global longitudinal strain, IVST = Interventricular septal wall thickness, LV = Left ventricular, LVIDd = LV internal diameter at end-diastole, LVIDs = LV internal diameter at end-systole, MFS = Midwall fractional shortening, PP= pulse pressure, PWT = Posterior wall thickness, RWTd = relative diastolic wall thickness, LAVi= left atrial volume index, LVEF= LV ejection fraction, LVMi= LV mass index.

Table 3. Correlations of LV GLS and PP in the pooled population.

Dependent variable	Correlate	R	P value
*GLS (%)	Age (years)	-0.03	0.718
	BMI (kg/m²)	-0.22	0.008
	Systolic BP (mmHg)	-0.28	0.001
	Diastolic BP (mmHg)	-0.18	0.027
	Mean BP (mmHg)	-0.24	0.004
	PP (mmHg)	-0.24	0.004
	LVMi (g/m^{2.7})	-0.10	0.217
	RWTd	-0.12	0.149
	E/A ratio	0.10	0.232
	Average e'	0.18	0.026
	E/e' ratio	-0.12	0.141

Dependent variable	Correlate	R	Pvalue
*PP	Age (years)	0.32	0.001
	BMI (kg/m²)	0.07	0.418
	GLS (%)	-0.24	0.004
	LVMi (g/m^{2.7})	0.25	0.002
	RWTd	0.14	0.102
	E/A ratio	-0.27	0.001
	Average e'	-0.23	0.005
	E/e' ratio	0.24	0.003

Abbreviations as in Table 1 and 2

*Values of GLS considered as “positive” (sign +) to build the associations in order to homogenize the results of analyses and strengthen their clinical meaning: the higher values the better strain deformation independent on the plus/minus sign.

Table 4. Multiple linear regression analysis in the pooled population Model 1

Dependent variable	Correlate	Standardized β coefficient	p value	Variance Inflation Factor
*GLS (%)	Age (years)	-0.056	0.539	1.199
	BMI (kg/m ²)	-0.198	0.025	1.095
	Highest PP tertile (mmHg)	-0.202	0.020	1.123
	LV mass index (g/m ^{2.7})	-0.030	0.969	1.100
	E/e' ratio	-0.057	0.535	1.271

Cumulative $R^2 = 0.113$, SEE =2.3%, p<0.01

Model 2

Dependent variable	Correlate	Standardized β coefficient	p value	Variance Inflation Factor
*GLS (%)	Age (years)	-0.017	0.845	1.130
	BMI (kg/m ²)	-0.182	0.040	1.109
	highest SBP tertile (mmHg)	-0.159	0.069	1.086
	LV mass index (g/m ^{2.7})	-0.013	0.882	1.285
	E/e' ratio	-0.041	0.662	1.098

Cumulative $R^2 = 0.101$, SEE =2.2 %, p<0.02

Abbreviations as in Tables 1 and 2.

*Values of GLS considered as “positive” (sign +) to build the associations in order to homogenize the results of analyses and strengthen their clinical meaning: the higher values the better strain deformation independent on the plus/minus sign.

Third Study: Background

Third study enrolled population of the Campania Salute Network registry and it was published on Journal Human Hypertension, 2015 Sep 10. The study evaluated predictors of progression toward isolated systolic hypertension in patients with systo-diastolic hypertension. We studied 7801 hypertensive patients without cardiovascular disease and/or chronic kidney failure, with at least 6-months follow-up period. Prevalence of isolated systolic hypertension was 21%. Patients with isolated systolic hypertension were older, with higher percentage of female sex, with longer history of hypertension and higher incidence of diabetes. Left ventricular mass, arterial stiffness, relative wall thickness, and intima-media thickness were also higher in patients with isolated systolic hypertension. Our findings suggest that isolated systolic hypertension is a manifestation of atherosclerotic disease worsening on target organ damages. It should be done more efforts to prevent the progression toward isolated systolic hypertension through more aggressive antihypertensive treatments, especially in subjects with phenotype at risk.

Third Study:

Identification of Phenotypes at Risk of Transition from Diastolic Hypertension to Isolated Systolic Hypertension

Abstract

Little is known about the potential progression of hypertensive patients towards isolated systolic hypertension (ISH) and about the phenotypes associated with the development of this condition. Aim of this study was to detect predictors of evolution towards ISH in patients with initial systolic-

diastolic hypertension. We selected 7,801 hypertensive patients free of prevalent cardiovascular diseases or severe chronic kidney disease, and with at least 6-month follow-up from the Campania Salute Network. During 55 ± 44 months of follow-up, incidence of ISH was 21%. Patients with ISH at the follow-up were significantly older ($p < 0.0001$) had longer duration of hypertension, higher prevalence of diabetes and were more likely to be women (all $p < 0.0001$). They exhibited higher baseline left ventricular mass index, arterial stiffness (Pulse Pressure/Stroke index), relative wall thickness, and carotid intima-media thickness (all $p < 0.001$). Independent predictors of incident ISH were older age (OR=1.14/5 years), female gender (OR=1.30), higher baseline systolic blood pressure (OR=1.03/5 mmHg), lower diastolic blood pressure (OR=0.89/5 mmHg), longer duration of hypertension (OR=1.08/5 months), higher left ventricular mass index (OR=1.02/5g \times m^{-2.7}), arterial stiffness (OR=2.01), relative wall thickness (OR=1.02), intima-media thickness (OR=1.19/mm; all $p < 0.0001$), independently of antihypertensive treatment, obesity, diabetes and fasting glucose ($p > 0.05$). Our findings suggest that ISH is a sign of aggravation of the atherosclerotic disease already evident by the target organ damage. Great efforts should be paid to prevent this evolution and prompt aggressive therapy for arterial hypertension should be issued before the onset of target organ damage, to reduce global CV risk.

KEY WORDS : hypertension, blood pressure, ventricular mass, carotid intima-media thickness, aging.

Background

Systolic blood pressure (SBP) increases with ageing (1;2), in relation to environmental stimuli (3). The age-related increase in SBP is also associated with decline of diastolic BP (DBP), mainly due

to loss of elasticity and consequent stiffening of conduit arteries (1-4), often producing isolated systolic hypertension (ISH)(4).

In the past, ISH has been considered almost as a physiologic condition, but in more recent decades, several studies have provided evidence that elevated SBP is an independent predictors of adverse cardiovascular (CV) outcomes, even more potent than elevated DBP, and that aggressive treatment of ISH might reduce hospitalization and mortality for CV causes (5-7). It has been calculated that for every 10 mmHg increase in SBP there is a 26% increase in overall mortality (7).

Although some information is available on characteristics of subjects from a general population who develop ISH (8), little is known on the possible evolution towards ISH in treated hypertensive patients initially presenting with diastolic or systolic-diastolic hypertension.

Accordingly, the present study was designed to assess whether and in which circumstances systolic-diastolic or isolated diastolic hypertension progresses into ISH. We focused on the identification of potential predictors of this progression in a large outpatient hypertensive population sample from our tertiary care center.

Methods

Patients

The Campania Salute Network (CSN) is an open registry collecting information from a network of 60 general practitioners and 23 community hospitals networked with the Hypertension Research Center of the Federico II University Hospital (Naples, Italy). The database generation of the CSN was approved by the Federico II University Hospital Ethic Committee. Signed informed consent was obtained from all the participants to use data for scientific purposes. Detailed characteristics of

this population have been previously reported (9-10). The database included over 12,000 patients, of whom 10,254 had confirmed arterial hypertension.

For the present study, we selected 7,801 patients with systolic-diastolic or isolated diastolic hypertension and with at least 6-month follow-up. The presence of ISH at baseline was an exclusion criteria for our selection. Moreover, all patients were free of prevalent CV disease (defined as previous myocardial infarction, angina or procedures of coronary revascularization, and/or history of stroke) and without chronic kidney disease more than stage 3. In the CSN, both prevalent and incident CV disease were adjudicated by an internal Committee for Event Adjudication and was based on patient history, contact with the reference general practitioner, and clinical records documenting occurrence of disease.

All hypertensive patients of the network underwent baseline echocardiograms and ultrasound evaluation of carotid arteries.

Protocol and Definitions

During baseline and follow-up visits, blood pressure, heart rate, body mass index (BMI), lipid and glucose profile were measured by standard methods. Diabetes was defined according to the American Diabetes Association criteria (11). Obesity was defined by $BMI \geq 30$. (12) Glomerular filtration rate (GFR) was estimated using serum creatinine and simplified Modification of Diet in Renal Disease (MDRD) equation (13). According to GFR values, we excluded patients with higher than stage II chronic kidney disease (CKD), meaning a $GFR < 59 \text{ mL/min/1.73 m}^2$ in KDOQI classification (13). BP was measured at the clinical visit with a digital sphygmomanometer (OMRON M7). In patients with frequent arrhythmias or atrial fibrillation we adopted a aneroid sphygmomanometer (Erka Perfect) calibrated every 6 months. Following current guidelines, the

blood pressure was measured 3 times in the sitting position after 5 minutes rest, and the average of the 2 last measurements was taken as the office BP.

Diastolic hypertension was defined as diastolic BP \geq 90 mmHg in at least 2 consecutive visits combined or not with systolic BP \geq 140 mmHg (systolic-diastolic hypertension) . Diagnosis of follow-up ISH was made at the time of the last available outpatient visit, according to European Guidelines (systolic BP \geq 140 mmHg with diastolic BP $<$ 90 mmHg). (14).

Cardiac Ultrasounds

Patients underwent M-mode and 2D-echocardiography, using a dedicated ultrasound machine (SONOS 5500; Philips, Andrews, Maryland, USA). Measurements were performed as previously reported (15;16), according to the American Societies of Echocardiography / European Association of Echocardiography (ASE/EAE) Recommendations (17) .

Left ventricular mass (LVM) was measured at end diastole and normalized for body height in meters to the power of 2.7 (LVMi).(18). Left ventricular hypertrophy (LVH) was defined as LVMi \geq 49.2 g/m^{2.7} in men and \geq 46.7 g/m^{2.7} in women. (18). Relative wall thickness (RWT) was calculated as posterior wall thickness/left ventricular end-diastolic radius (19). Pulse pressure (PP) to stroke index (SVi, by z-derived, normalized by height^{2.04}) (20;21), was used as a crude estimate of arterial stiffness.

Carotid Ultrasound

Carotid ultrasound was carried out in the supine position with the neck extended in mild rotation. The scanning protocol was performed with an ultrasound device (SONOS 2500/5500, HP, Philips) equipped with a 7.5 MHz high-resolution transducer with an axial resolution of 0.1 mm. Examinations were recorded on S-VHS videotapes and then analyzed off-line. The maximal arterial

intima-media thickness (IMT) was estimated offline, including the right and the left, near and far distal common carotid (1 cm), bifurcation, and proximal internal carotid artery, and using an image-processing dedicated workstation (MediMatic) as previously reported in detail (22).

Statistical analysis

Data were analyzed using SPSS20 and expressed as means \pm 1 SD. Descriptive statistics were performed using ANOVA and χ^2 distribution. To account for antihypertensive therapy, single classes of medications, including anti-renin-angiotensin system (RAS, i.e. ACE inhibitors and/or AT1 receptor antagonists), calcium-channel blockers (CCBs), β -blockers, and thiazide diuretics, were dichotomized according to their overall use during the individual follow-up, based on the frequency of prescription during the control visits. Thus, all medications prescribed for more than 50% of control visits were considered as covariates in logistic regression analysis. To isolate independent predictors of incident ISH we used binary logistic regression, using backward stepwise selection of main potential confounders including age, gender, diabetes, obesity, baseline BP, and duration of hypertension. In a second step, the markers of preclinical CV disease (LVMi, RWT, IMT, PP/SVi) were added to the first model. Finally, the classes of antihypertensive medications were forced into the model as a third step in the hierarchical procedure. A two-tailed $p < 0.05$ was considered significant.

Results

The median follow-up was 46 months (IQR=24-89 months). At the the time of the last outpatient visit, 1339 patients (17%) exhibited ISH, 51% of whom were women. Moreover, among our hypertensive patients we could identify 483 cases of isolated diastolic hypertension (IDH), 32% of whom were women, interestingly none of IDH patients developed ISH.

The initial demographic and clinical characteristics of patients with or without follow-up progression to ISH are listed in **Table 1**. As shown in this table, patients developing ISH were older, more often women and diabetic (all $p < 0.0001$) and had higher initial systolic and lower diastolic BP, producing a clear difference in pulse pressure. Duration of hypertension was also significantly greater in patients progressing to ISH all $p < 0.0001$). The two groups had not significant differences in heart rate, BMI, average number of antihypertensive medications and prevalence of smokers. Fasting glucose was higher and GFR lower in patients progressing to ISH (both $p < 0.0001$), whereas lipid profile and electrolytes were similar in the two groups.

Patient developing ISH exhibited higher baseline LV internal dimension, LVMI, RWT, arterial stiffness, and IMT than those without incident ISH (**Table 2**, all $p < 0.001$). Accordingly, the prevalence of baseline carotid plaque was also significantly greater in patients with (55%) than in those without (41%) incident ISH (OR=1.80 [1.57-2.05], $p < 0.0001$). In multivariable logistic regression, probability of progression to ISH was independently predicted by female gender ($p < 0.001$), older age, higher baseline SBP, lower DBP, longer duration of hypertension, higher values of baseline LVMI, RWT, PP/SVi, IMT (all $p < 0.0001$) and the lack of anti-RAS (ACE-inhibitors and/or angiotensin receptor blockers) prescription ($p < 0.04$), with no significant effect for diabetes, BMI and other classes of antihypertensive medications (**Table 3**). Interestingly the association of incident ISH with diabetes was significant (OR=1.26, 1.03-1.53, $p < 0.02$) until markers of CV damage were added to the model. Forcing classes of anti-hypertensive medications did not change the phenotypic profile at risk of evolution toward ISH. Classes of anti-hypertensive therapy were not independently related to development of ISH.

Discussion

This analysis demonstrate that in the context of arterial hypertension, the evolution toward ISH is actually a progression and can be predicted by a number of characteristics that define a specific phenotype at risk. Hypertensive patients evolving more often to ISH are older women with higher pulse pressure, signs of target organ damage, specifically increased LVMi, concentric LV geometry, and increased arterial stiffness. Our findings also suggest that transformation of a combined systolic-diastolic hypertension into ISH is related to the progression of arteriosclerotic disease, further reducing distensibility and elastic recoil of conduit arteries. ISH is the most common hypertension subtype for patients aged between 50 and 59 years, and it is the overwhelmingly dominant hypertensive subtype in the sixth decade of life. (23) ISH is characterized by elevated systolic BP in the presence of normal or decreased diastolic BP and it is associated with substantially increased pulse pressure and with an increased risk for adverse CV outcomes. In the Framingham Heart Study, systolic BP was a better independent predictor of CV risk than diastolic BP, particularly in patients over 50 years. (24;25) Staessen et al. (6) reported that in elderly patients with ISH, risk of death was associated positively with systolic BP and negatively with diastolic BP.

In the Framingham Heart Study population, (8) including subjects free of anti-hypertensive therapy and CV disease, according to baseline BP values, the group which had highest probability to develop ISH was the one which had normal or high-normal basal BP compared to the group that had basal systo-diastolic hypertension. The best independent clinical risk factors for new-onset ISH were age, female gender, and increased BMI during follow-up. In contrast with the Framingham population, (8) we studied patients with diastolic hypertension with or without high systolic BP, on antihypertensive treatment, also considering the impact of treatment and of markers of preclinical disease. Similar to the Framingham Heart Study, aging and female sex were two important

characteristics for evolution toward ISH. Another important difference from our study is that in the Framingham Heart Study the condition of preclinical CV disease (26) was not considered. This difference is substantial, and explains why we did not find an independent effect of diabetes and obesity, which was reported in the Framingham Heart Study. In our logistic model we considered both risk factors, but also the clinically unapparent consequences of exposition to those risk factors. Our analysis suggests that concentric LVH, increased carotid IMT and high arterial stiffness, albeit in the presence of diastolic hypertension, already express CV conditions that will progress to ISH. Our findings indicate that once the organ damage is established, the direct link between exposition to risk factors and overt CV disease is interrupted. Accordingly, ISH might be considered a further step in the progression from atherogenic risk factors exposition to CV adverse events, proposed by Devereux and Aldermann (26). This progression seems to be the result of the progressive stiffening of conduit arterial system, in part related to age, but also to the greater susceptibility to, and/or to the greater severity of, atherosclerotic disease, documented by the more severe target organ damage. Interestingly, women are more exposed than men to this progression, a finding that needs to be examined in depth. This scenario is consistent with the evidence that ISH is the most severe form of hypertension (6) and also more difficult to control than diastolic BP. Normalization of systolic BP in the context of ISH is a difficult challenge (27). It is possible that a greater effort should be paid to prevent progression to ISH. Our findings support current recommendations by guidelines, (14;28;29) to prompt aggressive therapy for arterial hypertension before the onset of target organ damage, to reduce global CV risk. This strategy might be very important to control incidence of ISH especially in elderly female patients.

References

1. Franklin SS, Gustin W, Wong ND, Larson MG, Weber MA, Kannel WB et al. Hemodynamic patterns of age-related changes in blood pressure: The Framingham Heart Study. *Circulation* 1997;96:308–315.
2. Danaei G, Finucane MM, Lin JK, Singh GM, Paciorek CJ, Cowan MJ et al. Global Burden of Metabolic Risk Factors of Chronic Diseases Collaborating Group (Blood Pressure). National, regional, and global trends in systolic blood pressure since 1980: systematic analysis of health examination surveys and epidemiological studies with 786 country-years and 5.4 million participants. *Lancet*. 2011 Feb 12;377(9765):568-77.
3. Timio M, Verdecchia P, Venanzi S, Gentili S, Ronconi M, Francucci B et al.. Age and blood pressure changes. A 20-year follow-up study in nuns in a secluded order. *Hypertension* 1988;12(4):457-461
4. O'Rourke MF, Nichols WW. Aortic diameter, aortic stiffness, and wave reflection increase with age and isolated systolic hypertension. *Hypertension*. 2005;45(4):652-8.
5. O'Donnell CJ, Ridker PM, Glynn RJ, Berger K, Ajani U, Manson JE et al. Hypertension and borderline isolated systolic hypertension increase risks of cardiovascular disease and mortality in male physicians. *Circulation*. 1997 Mar 4;95(5):1132-7.
6. Staessen JA, Gasowski J, Wang JG, Thijs L, Den Hond E, Boissel JP et al. Risks of untreated and treated isolated systolic hypertension in the elderly: meta-analysis of outcome trials. *Lancet*. 2000 Mar 3;357(9257):724.
7. Staessen JA, Fagard R, Thijs L, Celis H, Arabidze GG, Birkenhäger WH et al. Randomised double-blind comparison of placebo and active treatment for older patients

- with isolated systolic hypertension. The Systolic Hypertension in Europe (Syst-Eur) Trial Investigators. *Lancet*. 1997 Sep 13;350(9080):757-64.
8. Franklin SS, Pio JR, Wong ND, Larson MG, Leip EP, Vasan RS, Levy D. Predictors of new-onset diastolic and systolic hypertension: the Framingham Heart Study. *Circulation*. 2005 Mar 8;111(9):1121-7.
 9. Izzo R, de Simone G, Chinali M, Iaccarino G, Trimarco V, Rozza F et al. Insufficient control of blood pressure and incident diabetes. *Diabetes Care*. 2009 May;32(5):845-50.
 10. De Luca N, Izzo R, Iaccarino G, Malini PL, Morisco C, Rozza F et al.. The use of a telematic connection for the follow-up of hypertensive patients improves the cardiovascular prognosis. *J Hypertens*. 2005 Jul;23(7):1417-23.
 11. American Diabetes Association. Standards of medical care in Diabetes-2014. *Diabetes Care* 2014 Jan;37 Suppl 1: S14-80
 12. Clinical guidelines on the identification, evaluation, and treatment of overweight and obesity in adults: executive summary. Expert Panel on the Identification, Evaluation, and Treatment of Overweight in Adults.. *Am J Clin Nutr*. 1998 Oct; 68(4) 899-917.
 13. National Kidney Foundation. K/DOQI clinical practice guidelines for chronic kidney disease: evaluation, classification, and stratification. *Am J Kidney Dis*. 2002 Feb;39(2 Suppl 1):S1-266.
 14. ESH/ESC Task Force for the Management of Arterial Hypertension. 2013 Practice guidelines for the management of arterial hypertension of the European Society of Hypertension (ESH) and the European Society of Cardiology (ESC): ESH/ESC Task Force for the Management of Arterial Hypertension. *J Hypertens*. 2013 Oct;31(10):1925-38.

15. de Simone G, Izzo R, Chinali M, De Marco M, Casalnuovo G, Rozza F et al. Does information on systolic and diastolic function improve prediction of a cardiovascular event by left ventricular hypertrophy in arterial hypertension? *Hypertension*. 2010 Jul;56(1):99-104.
16. Izzo R, de Simone G, Trimarco V, Gerds E, Giudice R, Vaccaro O et al. Hypertensive target organ damage predicts incident diabetes mellitus. *Eur Heart J*. 2013 Nov;34(44):3419-26.
17. Lang RM, Bierig M, Devereux RB, Flachskampf FA, Foster E, Pellikka PA et al. Recommendations for chamber quantification: a report from the American Society of Echocardiography's Guidelines and Standards Committee and the Chamber Quantification Writing Group, developed in conjunction with the European Association of Echocardiography, a branch of the European Society of Cardiology. *J Am Soc Echocardiogr* 2005;18:1440-1463.
18. de Simone G, Daniels SR, Devereux RB, Meyer RA, Roman MJ, de Divitiis O et al. Left ventricular mass and body size in normotensive children and adults: assessment of allometric relations and impact of overweight. *J Am Coll Cardiol*. 1992 Nov 1;20(5):1251-60.
19. Ganau A, Devereux RB, Roman MJ, de Simone G, Pickering TG, Saba PS et al. Patterns of left ventricular hypertrophy and geometric remodeling in essential hypertension. *J Am Coll Cardiol*. 1992 Jun;19(7):1550-8.
20. de Simone G, Devereux RB, Ganau A, Hahn RT, Saba PS, Mureddu GF et al. Estimation of left ventricular chamber and stroke volume by limited M-mode

echocardiography and validation by two-dimensional and Doppler echocardiography. *Am J Cardiol* 1996 Oct 1;78(7):801-7.

21. de Simone G, Devereux RB, Daniels SR, Mureddu G, Roman MJ, Kimball TR et al. Stroke volume and cardiac output in normotensive children and adults. Assessment of relations with body size and impact of overweight. *Circulation* 1997 Apr 1;95(7):1837-1843.
22. Casalnuovo G, Gerdtz E, De Simone G, Izzo R, De Marco M, Giudice R et al. Arterial stiffness is associated with carotid atherosclerosis in hypertensive patients (the campania salute network). *Am J Hypertens* 2012 Jul; 25(7):739-745.
23. Franklin SS, Milagros J. Jacobs, Nathan D. Wong, Gilbert J. L'Italien and Pablo Lapuerta. Predominance of Isolated Systolic Hypertension Among Middle-Aged and Elderly US Hypertensives: Analysis Based on National Health and Nutrition Examination Survey (NHANES) III. *Hypertension*. 2001 Mar;37(3):869-874
24. Kannel WB, Gordon T, Schwartz MJ. Systolic versus diastolic blood pressure and risk of coronary heart disease. The Framingham Study. *Am J Cardiol* 1971 Apr; 27(4):335±346.
25. Kannel WB, Dawber TR, Sorlie P, Wolf PA. Components of blood pressure and risk of atherothrombotic brain infarction: the Framingham Study. *Stroke* 1976 Jul-Aug; 7(4):327±331.
26. Devereux RB, Alderman MH. Role of preclinical cardiovascular disease in the evolution from risk factor exposure to development of morbid events. *Circulation* 1993 Oct; 88:1444-1455.

27. Fagard RH, Staessen JA, Thijs L, Gasowski J, Bulpitt CJ, Clement D et al. Response to antihypertensive therapy in older patients with sustained and nonsustained systolic hypertension. Systolic Hypertension in Europe (Syst-Eur) Trial Investigators. *Circulation*. 2000 Sep 5;102(10):1139-44.
28. De Simone G, Devereux RB, Izzo R, Girfoglio D, Lee ET, Howard BV et al. Lack of reduction of left ventricular mass in treated hypertension: the strong heart study. *J Am Heart Assoc*. 2013 Jun 6; 2(3)
29. Weber MA, Schiffrin EL, White WB, Mann S, Lindholm LH, Kenerson JG et al. Clinical practice guidelines for the management of hypertension in the community a statement by the American Society of Hypertension and the International Society of Hypertension. *J Hypertens*. 2014 Jan;32(1):3-15.

Tables

Table 1. Baseline demographic and clinical characteristics dichotomized by evidence of follow-up ISH

	No follow-up ISH (n = 6462)	Follow-up ISH (n = 1339)	p
Age, years	51.2±10.7	56.8±11.0	<0.0001
Women, %	41.8	50.9	<0.0001
Body Mass Index, kg/m ²	27.8±4.1	27.8±4.2	ns
systolic BP, mmHg	157.4±19.4	162.1±19.5	<0.0001
diastolic BP, mmHg	100.5±9.3	99.4±8.1	<0.0001
Heart rate, bpm	71.8±11.8	71.9±11.9	ns
Duration of hypertension, years	10.7±7.5	13.4±8.9	<0.0001
Average number of antihypertensive medications	1.7±1.1	1.8±1.1	ns
Diabetes, %	11.3	18.9	<0.0001
Smoking habits, %	48.6	45.9	ns
Fasting glucose, mmol/L	5.44±1.17	5.61±1.44	<0.0001
Total cholesterol, mmol/L	5.3±1.0	5.4±1.0	ns
HDL-cholesterol, mmol/L	1.3±0.3	1.3±0.3	ns
Triglycerides, mmol/L	1.5±0.9	1.5±0.8	ns
GFR, mL/min/1.73 m ²	79.5±18.0	77.1±18.3	<0.0001
Sodium, mmol/L	141.0±3.2	141.2±3.3	ns
Potassium, mmol/L	4.4±0.4	4.4±0.4	ns

Values are means ± SD. BP = blood pressure; HDL = High-density lipoprotein; GFR = Glomerular Filtration Rate.

Table 2. Baseline target organ damage by evidence of follow-up of ISH

	No follow-up ISH (n = 6462)	Follow-up ISH (n = 1339)	P
LVMi, g/m ^{2.7}	47.4±9.1	49.6±9.8	<0.0001
LVIDD/ht, cm/m	2.96±0.19	3.00±0.20	<0.0001
Relative Wall Thickness	0.38±0.03	0.39±0.04	<0.001
PP/SVi, mmHg/ml/beat*m ^{2.04}	2.3±0.6	2.6±0.7	<0.0001
Max IMT, mm	1.5±0.7	1.8±0.8	<0.0001

Values are means ± SD. LVMi = Left Ventricular Mass index; PP/SVi = Pulse Pressure/Stroke Volume index; IMT = Intima-Media Thickness, LVIDD/ht = Left Ventricular Internal Diastolic Diameter/height.

Table 3 Independent predictors of follow-up ISH at logistic regression

Predictors	OR	95% C.I.for OR		p
		Lower-	Upper	
Female sex	1.29	1.12-	1.50	<0.001
Age (× 5 yrs)	1.14	1.10-	1.18	<0.0001
Systolic BP (× 5 mmHg)	1.03	1.01-	1.06	<0.0001
Diastolic BP (× 5 mmHg)	0.89	0.83-	0.95	<0.0001
Duration of hypertension (×5 months)	1.11	1.06-	1.16	<0.0001
LV mass index (× 5 g/m ^{2.7})	1.08	1.04-	1.12	<0.0001
Relative wall thickness	0.02	0.01-	0.15	<0.0001
PP/SVi	1.99	1.77-	2.23	<0.0001
Carotid Intima media thickness (mm)	1.19	1.07-	1.33	<0.0001
Anti-RAS prescription	0.85	0.73-	0.99	<0.04

Values are means ± SD. BP = Blood Pressure; LV = Left Ventricular; PP/SVi = Pulse Pressure/Stroke Volume index; Anti-RAS = ACE-inhibitors and/or angiotensin receptor blockers.

Diabetes, BMI and other classes of antihypertensive medications did not enter into the final model (p>0.05).

Figures

Figure 1 displays the relative contribution of all covariates used in the complete logistic model: the initial PP/SVi was by far the most important predictor of ISH followed by age, with the other significant components impacting similarly.

